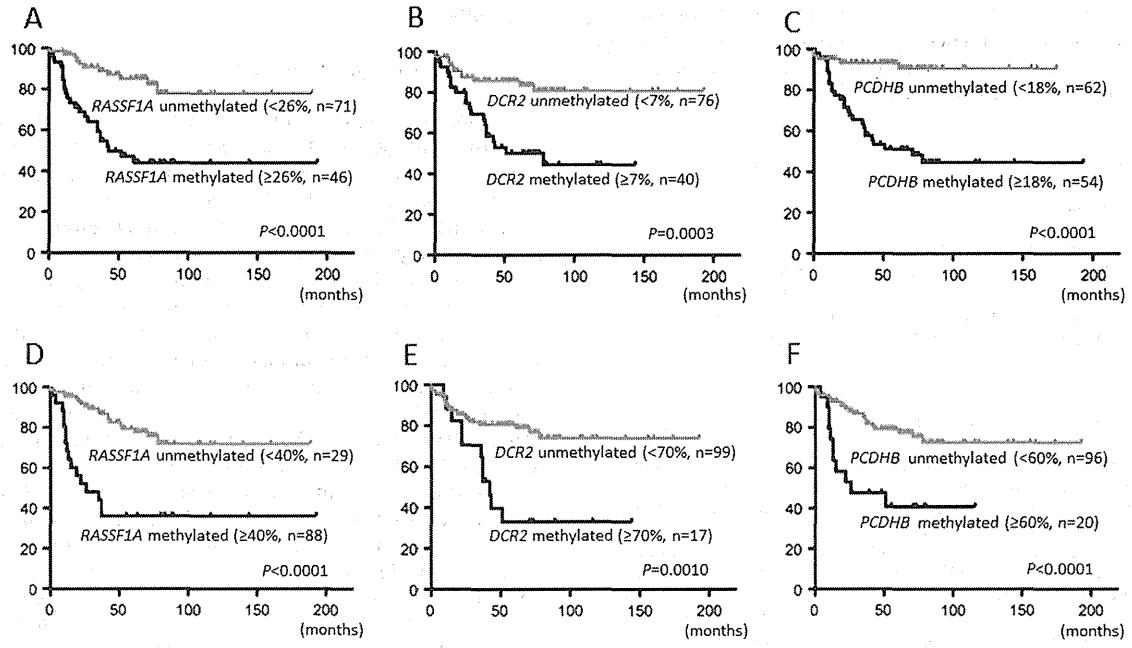

Fig. 1. Overall survival curves for infants and children diagnosed clinically and classified by the cut-off value in tumors determined by ROC analysis; (A) *RASSF1A*, 26% [$P < 0.0001$, hazard ratio (HR) 4.634, 95% confidence interval (95%CI) 2.3–9.3]; (B) *DCR2*, 7% ($P = 0.0003$, HR 3.91, 95%CI 1.9–8.2); (C) *PCDHB*, 18% ($P < 0.0001$, HR 5.35, 95%CI 2.7–10.8), and by the dose–response relationship; (D) *RASSF1A*, 40% ($P < 0.0001$, 7.89, 95%CI 3.3–19.2; (E) *DCR2*, 70% ($P = 0.001$, 5.34, 95%CI 2.0–14.5); (F) *PCDHB*, 60% ($P < 0.0001$, 6.11, 95%CI 2.2–16.9).

Table 1
Association between *RASSF1A*, *CASP8*, *DCR2*, and *PCDHB* methylation and stage of the disease.

	Group A1 (≤18 m)	Group A2 (≤18 m)	Group B (>18 m)		Group A2 (≤18 m)	Group B (>18 m)
RASSF1A (cMSP)				*RASSF1A* (qMSP)		
Total (methyl versus unmethyl)	NS	S (0.018)	S (5.49E−05)		ROC, S (0.029); DRR., NS	ROC, S (0.008); DRR., S (0.022)
Diploidy (methyl versus unmethyl)	S (0.029)	M (0.052)	S (0.006)		ROC, NS; DRR., NS	ROC, M (0.078); DRR., NS
Triploidy (methyl versus unmethyl)	NS	NS	S (3.12E−03)		ROC, NS; DRR, NA	ROC, M (0.080); DRR., NS
CASP8 (cMSP)						
Total (methyl versus unmethyl)	NS	M (0.090)	S (0.026)			
Diploidy (methyl versus unmethyl)	NA	NS	NS			
Triploidy (methyl versus unmethyl)	NS	NA	NS			
DCR2 (cMSP)				*DCR* (qMSP)		
Total (methyl versus unmethyl)	NS	NS	S (5.06E−05)		ROC, NS; DRR, NA.	ROC, S (0.005); DRR., S (0.004)
Diploidy (methyl versus unmethyl)	NS	NS	S (0.003)		ROC, NS; DRR, NA	ROC, M (0.057); DRR., S (0.033)
Triploidy (methyl versus unmethyl)	NS	NA	S (0.017)		ROC, NA ; DRR, NA	ROC, S (0.048); DRR., NS
PCDHB				*PCDHB* (qMSP)		
Total (methyl versus unmethyl)					ROC, NS; DRR., NS	ROC, S (5.70E−06); DRR., M (0.051)
Diploidy (methyl versus unmethyl)					ROC, NS; DRR., NS	ROC, S (0.001); DRR., NS
Triploidy (methyl versus unmethyl)					ROC, NS; DRR, NS	ROC, S (0.003); DRR., NS

Group A1, infants found by mass-screening; Group A2, infants diagnosed clinically; Group B, children diagnosed clinically; m, month; cMSP, conventional methylation-specific PCR; qMSP, quantitative methylation-specific PCR; Methyl, methylated; unmethyl, unmethylated; NS, not significant; S, significant; M, marginally significant; NA, not applicable; ROC, ROC analysis; DRR, dose–response relationship analysis; Detailed data are shown in Supplementary Tables 2–7.

Please cite this article in press as: M. Haruta et al., *RASSF1A* methylation may have two biological roles in neuroblastoma tumorigenesis depending on the ploidy status and age of patients, Cancer Lett. (2014), http://dx.doi.org/10.1016/j.canlet.2014.03.022

Table 2
Association between *RASSF1A*, *CASP8*, *DCR2*, and *PCDHB* methylation and *MYCN* amplification.

	Group A1 (≤18 m)	Group A2 (≤18 m)	Group B (>18 m)		Group A2 (≤18 m)	Group B (>18 m)
RASSF1A (cMSP)				*RASSF1A* (qMSP)		
Total (methyl versus unmethyl)	NS	S (0.001)	S (0.002)		ROC, S (5.29E−06); DRR., S (8.97E−06)	ROC, S (0.003); DRR., S (0.001)
Diploidy (methyl versus unmethyl)	NS	S (0.005)	S (0.011)		ROC, S (0.002); DRR., S (0.001)	ROC, S (0.003); DRR., S (0.003)
Triploidy (methyl versus unmethyl)	NA	NA	NS		ROC, NA; DRR., NA.	ROC, M (0.08); DRR, NS
CASP8 (cMSP)						
Total (methyl versus unmethyl)	NS	S (1.94E−07)	S (0.002)			
Diploidy (methyl versus unmethyl)	NA	S (1.35E−04)	S (0.034)			
Triploidy (methyl versus unmethyl)	NA	NA	S (0.027)			
DCR2 (cMSP)				*DCR2* (qMSP)		
Total (methyl versus unmethyl)	NS	NS	NS		ROC, S (0.043); DRR., NA	ROC, NS; DRR., NS
Diploidy (methyl versus unmethyl)	NS	NS	NS		ROC, NS; DRR., NA.	ROC, NS; DRR., NS
Triploidy (methyl versus unmethyl)	NA	NA	NS		ROC, NA; DRR., NA.	ROC, NS; DRR., NS
PCDHB (cMSP)				*PCDHB (qMSP)*		
Total (methyl versus unmethyl)					ROC, S (2.34E−07); DRR., S (1.2E−04)	ROC, S (0.003); DRR., M (0.091)
Diploidy (methyl versus unmethyl)					ROC, S (5.86E−06); DRR., S (0.005)	ROC, S (0.036); DRR., S (0.032)
Triploidy (methyl versus unmethyl)					ROC, NA; DRR, NA.	ROC, NS; DRR., NS

Group A1, infants found by mass-screening; Group A2, infants diagnosed clinically; Group B, children diagnosed clinically; m, month; cMSP, conventional methylation-specific PCR; qMSP, quantitative methylation-specific PCR; Methyl, methylated; unmethyl, unmethylated; NS, not significant; S, significant; M, marginally significant; NA, not applicable; ROC, ROC analysis; DRR, dose–response relationship analysis; Detailed data are shown in Supplementary Tables 2–7.

children were at a more advanced stage than *DCR2*-unmethylated diploid and triploid tumors in children, respectively ($P = 0.003$ and $P = 0.017$), and the results were consistent with those obtained by quantitative MSP.

Quantitative MSP analysis disclosed that *PCDHB*-methylated diploid and triploid tumors were at more advanced stages than *PCDHB*-unmethylated diploid and triploid tumors, respectively, in children ($P = 0.001$ and $P = 0.003$). Such an association was not found between *PCDHB*-methylated and -unmethylated tumors in infants.

3.3. Correlation of methylation in the RASSF1A, CASP8, DCR2, and PCDHB genes with MYCN amplification

Because only 2 of 123 tumors found by mass-screening had *MYCN* amplification, further studies on the correlation were not conducted (Table 2). *RASSF1A* methylation detected by conventional MSP was associated with *MYCN* amplification in tumors in infants and children ($P = 0.001$ and $P = 0.002$). *CASP8* methylation was also associated with *MYCN* amplification in tumors in infants and children ($P = 1.94E{-}07$ and $P = 0.002$). In contrast, no association was found between *DCR2* methylation and *MYCN* amplification in tumors in infants and children. Quantitative MSP analysis in *RASSF1A* and *DCR2* methylation confirmed the findings. In addition, *PCDHB* methylation was also identified to have correlation with *MYCN* amplification in tumors of infants and children. The association between *RASSF1A* and *PCDHB* methylation and *MYCN* amplification was also indicated by different distributions of methylation percentages of *RASSF1A* and *PCDHB* between *MYCN*-amplified and –nonamplified tumors; however, different distributions of *DCR2* methylation percentages were not exhibited between the tumors in infants and children (Fig. 2).

We then classified tumors by the ploidy status, and found that none of the triploid tumors in infants had *MYCN* amplification. *RASSF1A* methylation was associated with *MYCN* amplification in diploid tumors in infants and children ($P = 0.005$ and $P = 0.011$), but not in triploid tumors in children. *DCR2* methylation was not associated with *MYCN* amplification in diploid and triploid tumors in children. Quantitative MSP analysis confirmed the association with *MYCN* amplification found in *RASSF1A*-methylated tumors, and no association found in *DCR2*-methylated tumors. *CASP8* methylation was associated with *MYCN* amplification in diploid tumors in infants ($P = 1.35E{-}04$) or in diploid and triploid tumors in children ($P = 0.034$ and $P = 0.027$). The correlation between *PCDHB* methylation and *MYCN* amplification was found in tumors of infants and children. When divided by the ploidy status, *RASSF1A* and *PCDHB* methylation was correlated with *MYCN* amplification in diploid, not triploid tumors in infants and children. *DCR2* methylation (>7%) was found only 3 of 53 tumors in infants; further study was not conducted. The correlation between *DCR2* methylation and *MYCN* amplification was not found in tumors of children.

3.4. Correlation between the methylation status of the RASSF1A, CASP8, DCR2, and PCDHB genes analyzed by conventional and quantitative MSP and overall survival

There was no prognostic significance of methylation of *RASSF1A*, *CASP8*, and *DCR2* in infants found by mass-screening because only two of 123 infants died of the disease (Table 3 and Supplementary Tables 2–4). When we combined infants and children clinically

Please cite this article in press as: M. Haruta et al., *RASSF1A* methylation may have two biological roles in neuroblastoma tumorigenesis depending on the ploidy status and age of patients, Cancer Lett. (2014), http://dx.doi.org/10.1016/j.canlet.2014.03.022

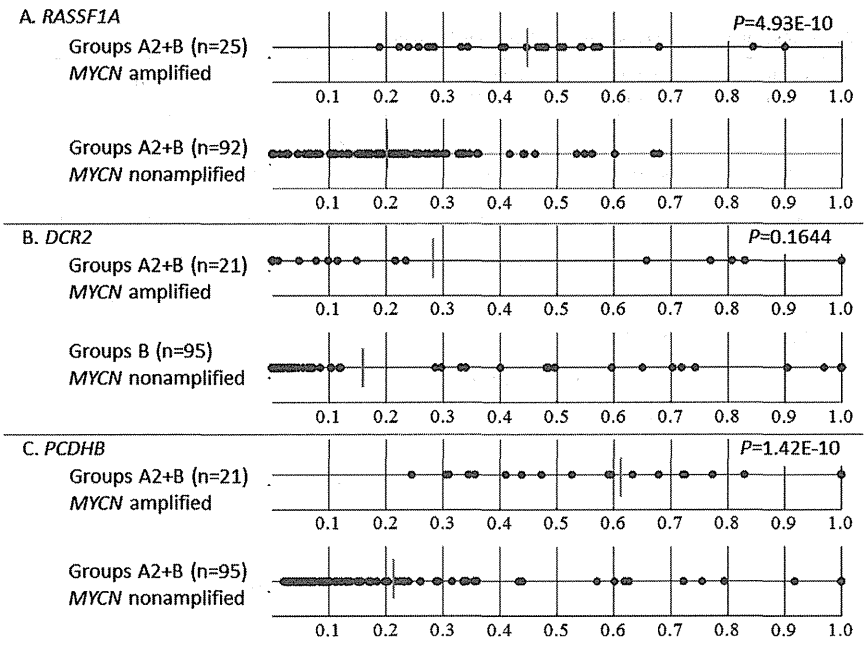

Fig. 2. The distribution of *RASSF1A*, *DCR2*, and *PCDHB* methylation percentages between *MYCN* amplified and *MYCN*-nonamplified tumors.

Table 3
Association between *RASSF1A*, *CASP8*, *DCR2*, and *PCDHB* methylation and overall survival.

	Group A1 (≤18 m)	Group A2 (≤18 m)	Group B (>18 m)		Group A2 (≤18 m)	Group B (>18 m)
RASSF1A (cMSP)				*RASSF1A* (qMSP)		
Total (methyl versus unmethyl)	NS	M (0.0705)	S (0.0331)		ROC, S (0.0001); DRR., S (0.0002)	ROC, S (0.0288); DRR., S (0.0060)
Diploidy (methyl versus unmethyl)	NS	S (0.0405)	NS		ROC, S (0.0057); DRR., S (0.0031)	ROC, NS; DRR., NS
Triploidy (methyl versus unmethyl)	NA	NS	NS		ROC, NA; DRR., NA	ROC, NS; DRR., S (0.0126)
CASP8 (cMSP)						
Total (methyl versus unmethyl)	NS	S (<0.0001)	NS			
Diploidy (methyl versus unmethyl)	NA	S (0.0027)	NS			
Triploidy (methyl versus unmethyl)	NA	NA	NS			
DCR2 (cMSP)				*DCR2* (qMSP)		
Total (methyl versus unmethyl)	NS	NA	M (0.0821)		ROC, S (0.0020); DRR., NA	ROC, NS; DRR., S (0.0360)
Diploidy (methyl versus unmethyl)	NA	NA	NS		ROC, S (0.0381); DRR., NA	ROC, NS; DRR., NS
Triploidy (methyl versus unmethyl)	NA	NA	S (0.0182)		ROC, NA; DRR., NA	ROC, NS; DRR., S (0.0164)
PCDHB (cMSP)				*PCDHB* (qMSP)		
Total (methyl versus unmethyl)					ROC, S (0.0101); DRR., S (<0.0001)	ROC, S (0.0218); DRR., NS
Diploidy (methyl versus unmethyl)					ROC, M (0.0609); DRR., S (0.0007)	ROC, NS; DRR., S (0.0451)
Triploidy (methyl versus unmethyl)					ROC, NA; DRR., NA	ROC, M (0.0850); DRR., NS

Group A1, infants found by mass-screening; Group A2, infants diagnosed clinically; Group B, children diagnosed clinically; m, month; cMSP, conventional methylation-specific PCR; qMSP, quantitative methylation-specific PCR; Methyl, methylated; unmethyl, unmethylated; NS, not significant; S, significant; M, marginally significant; NA, not applicable; ROC, ROC analysis; DRR, dose–response relationship analysis; Detailed data are shown in Supplementary Tables 2–7.

diagnosed, patients with a *RASSF1A*-, *CASP8*-, or *DCR2*-methylated tumor examined by conventional MSP had worse overall survival than patients with a *RASSF1A*-, *CASP8*-, or *DCR2*-unmethylated tumor, respectively ($P = 0.0015$, $P = 0.0003$, and $P = 0.0038$) (Fig. 3A–C).

When we further classified patients according to the ploidy status, infants with a *RASSF1A*-methylated diploid tumor had worse overall survival than infants with a *RASSF1A*-unmethylated diploid tumor ($P = 0.0405$); however, such an association was not found in infants with triploid tumors (Fig. 3D and F). In addition, infants with a *CASP8*-methylated diploid tumor had worse overall survival than infants with a *CASP8*-unmethylated diploid tumor ($P = 0.0027$). No significant difference was observed in overall

Please cite this article in press as: M. Haruta et al., *RASSF1A* methylation may have two biological roles in neuroblastoma tumorigenesis depending on the ploidy status and age of patients, Cancer Lett. (2014), http://dx.doi.org/10.1016/j.canlet.2014.03.022

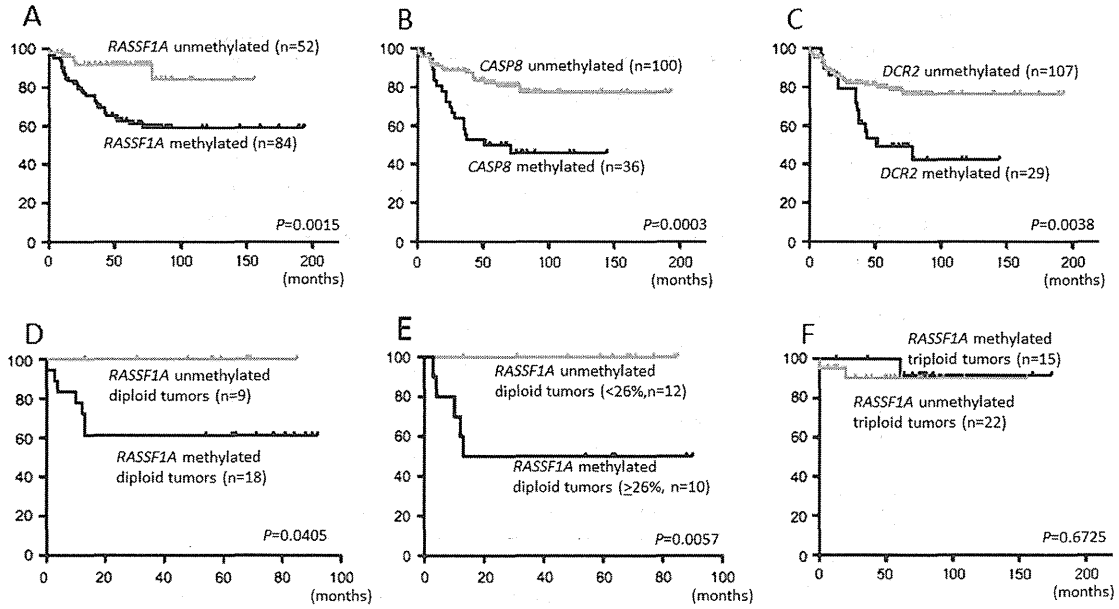

Fig. 3. Overall survival curves for infants and children diagnosed clinically and classified by the methylation status of *RASSF1A* (A), *CASP8* (B), and *DCR2* (C) examined by conventional MSP analysis. Overall survival curves for infants with a *RASSF1A*-methylated diploid tumor and those with a *RASSF1A*-unmethylated diploid tumor diagnosed clinically and examined by conventional MSP (D), or quantitative MSP (E) analysis, and for infants with a *RASSF1A*-methylated triploid tumor and those with a *RASSF1A*-unmethylated triploid tumor diagnosed clinically and examined by conventional MSP (F).

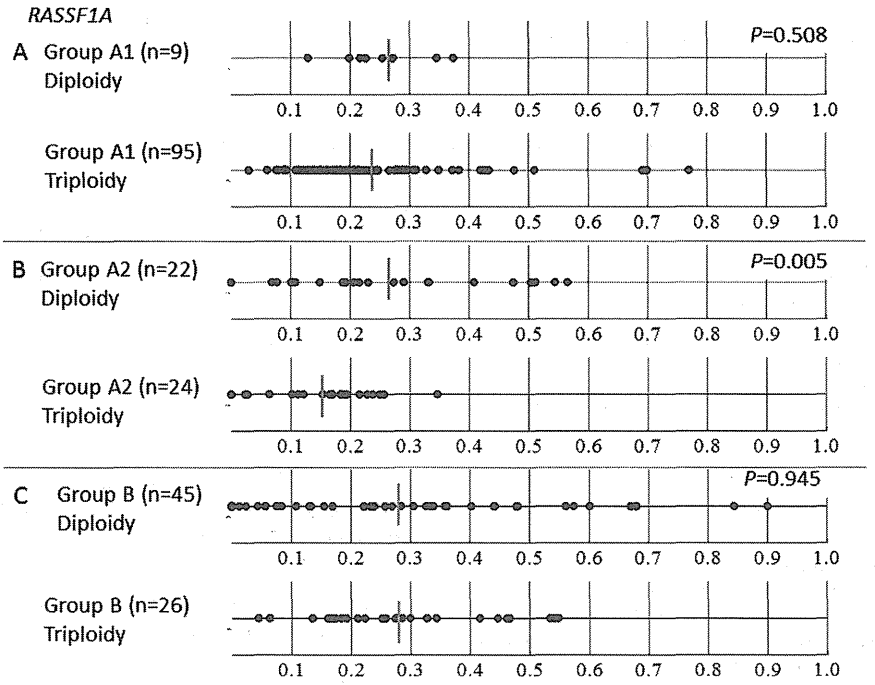

Fig. 4. The distribution of *RASSF1A* methylation percentages between diploid and triploid tumors in infants found by mass-screening (A), between diploid and triploid tumors in infants (<18 months) diagnosed clinically (B), and between diploid and triploid tumors in children (>18 months) (C).

survival between any two of the 4 types of tumors classified by the methylation status of *RASSF1A* or *CASP8* and the ploidy status in children. In contrast, children with a *DCR2*-methylated triploid tumor had worse overall survival than children with a *DCR2*-unmethylated triploid tumor ($P = 0.0182$).

When we analyzed *RASSF1A*, *DCR2*, and *PCDHB* methylation by quantitative MSP, an association between methylation of each gene and poor outcomes was identified in tumors of infants and children (Table 3). When we divided tumors according to the ploidy status, *RASSF1A* and *DCR2*, not *PCDHB* methylation was associated with a poor outcome in infants with a diploid, not triploid tumor. Interestingly, *RASSF1A* and *DCR2* methylation was correlated with a poor outcome in children with a triploid, not diploid tumor.

Please cite this article in press as: M. Haruta et al., *RASSF1A* methylation may have two biological roles in neuroblastoma tumorigenesis depending on the ploidy status and age of patients, Cancer Lett. (2014), http://dx.doi.org/10.1016/j.canlet.2014.03.022

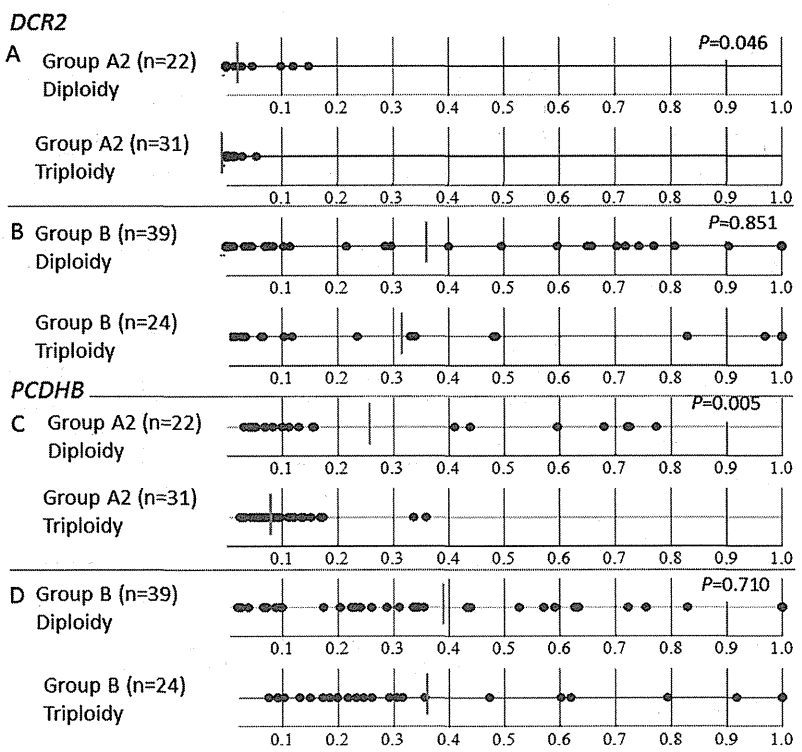

Fig. 5. The distribution of *DCR2* methylation percentages between diploid and triploid tumors in infants (<18 months) diagnosed clinically (A), and between diploid and triploid tumors in children (>18 months) (B). The distribution of *PCDHB* methylation percentages between diploid and triploid tumors in infants (<18 months) diagnosed clinically (C), and between diploid and triploid tumors in children (>18 months) (D).

Table 4
Multivariate analysis on 5 clinicopathological and genetic factors including *RASSF1A* methylation in 102 patients with neuroblastoma.

Prognostic factors	Relative risk (95%CI[a])	*P*-value	Relative risk (95%CI[a])	*P*-value
Age: ≤18 months versus > 18 months	2.07 (0.84–5.13)	0.1159	1.88 (0.75–4.70)	0.1754
Stage: 1, 2, 4S versus 3, 4	2.71 (0.79–9.27)	0.1116	2.88 (0.86–9.62)	0.0859
Ploidy: Triploidy versus diploidy	1.40 (0.65–3.01)	0.3940	1.26 (0.58–2.75)	0.5648
MYCN: Single copy versus amplification	3.19 (1.45–7.03)	0.0041	3.30 (1.55–7.00)	0.0019
RASSF1A [b]: Unmethylated (<26%) versus methylated (>26%)	1.55 (0.67–3.61)	0.3086		
RASSF1A [c]: Unmethylated (<40%) versus methylated (>40%)			2.19 (1.02–4.72)	0.0455

[a] 95%CI, 95% confidence interval.
[b] The cut-off value was determined by ROC analysis.
[c] The cut-off value was determined by the dose-response relationship.

3.5. The mean methylation percentage between diploid and triploid tumors in infants and children

The mean methylation percentage of *RASSF1A* was higher in diploid tumors than in triploid tumors of infants diagnosed clinically; however, such an association was not observed in tumors of infants found by mass-screening or children (Fig. 4). Likewise, the mean methylation percentage of *DCR2* or *PCDHB* was higher in diploid tumors than in triploid tumors of infants; however, such an association was not observed between diploid and triploid tumors in children (Fig. 5).

The difference in the methylation percentage of *RASSF1A* or *DCR2* between diploid and triploid tumors in infants, but not in children reflected the difference in outcomes between infants having a diploid tumor with or without *RASSF1A* or *DCR2* methylation ($P = 0.0057$ and $P = 0.0381$), but not between children having a diploid tumor with or without (Table 3). Interestingly, the difference in outcomes was observed between children having a triploid tumor with or without *RASSF1A* or *DCR2* methylation, but not between infants having a triploid tumor with or without; methylation percentages of *RASSF1A* or *DCR2* rarely exceeded cut-off values of 27% or 7% in triploid tumors in infants (Figs. 4 and 5).

3.6. Multivariate Cox proportional hazard regression analysis on 5 clinical and genetic factors in 102 patients clinically diagnosed

Multivariate analysis exhibited the *MYCN* amplification and *RASSF1A* methylation statuses were shown to be independent factors predicting poor outcome, but the *PCDHB* and *DCR2* methylation statuses were not (Table 4, and Supplementary Tables 8 and 9).

4. Discussion

The present study using conventional MSP found methylation of the *RASSF1A*, *CASP8*, and *DCR2* genes in 62%, 25%, and 21%, respectively, of 136 neuroblastoma samples diagnosed clinically. Previous studies reported methylation of *RASSF1A*, *CASP8*, and *DCR2* in

Please cite this article in press as: M. Haruta et al., *RASSF1A* methylation may have two biological roles in neuroblastoma tumorigenesis depending on the ploidy status and age of patients, Cancer Lett. (2014), http://dx.doi.org/10.1016/j.canlet.2014.03.022

Table 5
Incidences and associations between *RASSF1A*, *CASP8*, and *DCR2* methylation and disease stage, *MYCN* amplification, and overall or event-free survival.

	RASSF1A				*CASP8*				*DCR2*			
Studies	Incidence	Stage	*MYCN* amp.	Survival	Incidence	Stage	*MYCN* amp.	Survival	Incidence	Stage	*MYCN* amp.	Survival
Astuti et al. [14]	55%, 37/67	N. S.	N. S.	N. S.	40%, 24/60	N. D.	N. D.	N. D.				
Yang et al. [15]	70%, 39/56	N. S.	N. S.	OS, $P < 0.01$								
Banelli et al. [16]	84%, 26/31	N. D.	$P < 0.05$	OS, N. S.		N. D.	N. S.	N. D.	42%, 13/31	N. D.	N. S.	OS, $P < 0.03$
Lázcoz et al. [17]	83%, 29/35	N. D.	N. S.	N. D.	60%, 21/35	N. D.	N. S.	N. D.				
Yang et al. [18]	90%, 63/70	N. D.	N. D.	N. D.	56%, 39/70	N. D.	N. S.	OS, $P = 0.008$	44%, 31/70	N. D.	N. D.	OS, $P = 0.019$
Michalowski et al. [19]	93%, 42/45	N. D.	N. D.	N. S.	38%, 17/45	$P = 0.001$	N. S.	N. S.				
Misawa et al. [20]	94%, 64/68	N. S.	N. S.	N. S.								
Hoebeeck et al. [21]	71%, 29/41	N. S.	N. S.	OS and EFS, N. S.	56%, 20/36	N. S.	N. S.	EFS, $P = 0.038$				
Grau et al. [22]	66%, 54/82	$P = 0.024$	N. S.	EFS, $P = 0.003$ (intermediate risk)	52%, 43/8	$P < 0.001$	$P = 0.007$	OS, $P = 0.019$ EFS, $P = 0.002$				
Stutterheim et al. [23]	96%, 68/71	N. D.	St 1–3, $P = 0.006$ St 4, $P = 0.05$	OS, $P = 0.02$ (St 4 & > 1 y.)								
Kiss et al. [24]	61%, 23/38	N. D.	N. D.	N. D.	55%, 21/38	N. D.	N. S.	N. D.				
Teitz et al. [25]					62%, 26/42	N. S.	$P < 0.0001$	N. D.				
Takita et al. [26]					32%, 8/25	N. D.	N. S.	N. D.				
Gonzalez-Gomez et al. [27]					14%, 6/38	$P = 0.019$	$P = 0.0047$	N. D.				
Asada et al. [28]					19%, 26/140 20%, 30/152	N. D.	N. D.	OS $P = 0.002$ in Japanese $P = 0.0002$ in German				
van Noesel et al. [29]									70%, 39/56	N. D.	N. D.	N. D.
Yagyu et al. [30]									28%, 24/86	N. D.	N. D.	OS, $P = 0.008$ EFS, $P < 0.001$
Present study	62%, 84/136	<18 m, $P = 0.018$ >18 m, $P < 0.001$	$P < 0.001$	OS, $P = 0.0015$	27%, 36/136	<18 m $P = 0.090$ >18 m $P = 0.026$	$P = 0.0003$	OS, $P < 0.001$	21%, 29/136	<18 m, $P = 0.406$ >18 m, $P < 0.001$	$P = 0.149$	OS, $P = 0.0038$

N. S., not significant; N. D., not done; OS, overall survival; EFS, event-free survival; st, stage; 1 y., one year; Studies were cited in the Reference section.

55–96%, 14–62%, and 28–70% in 25–86 neuroblastoma samples (Table 5) [14–30]. The various results may have been affected by the location of primers for target genes and numbers of PCR cycles used for conventional and quantitative MSP analysis. We also evaluated *PCDHB* methylation, which was reported in a substantial number of neuroblastoma samples [31].

Regarding to methylation of the 4 genes and the stage distribution, *RASSF1A* methylation was associated with a more advanced stage in infants and children diagnosed clinically and in infants with a diploid tumor found by mass-screening, whereas *CASP8*, *DCR2*, and *PCDHB* methylation was associated with an advanced stage only in tumors of children (Table 1). The findings reflected that *RASSF1A* methylation was fairly common in neuroblastoma in infants, while *CSAP8*, *DCR2*, and *PCDHB* methylation was rare in tumors of infants, especially in triploid tumors.

Associations between *RASSF1A*, or *CASP8* methylation and *MYCN* amplification have been reported (Table 5) [14–28]. In addition, neuroblastoma with *PCDHB* methylation was reported to include all tumors with *MYCN* amplification, and associated with a poor outcome [31]. The present study exhibited that *RASSF1A*, *CASP8*, or *PCDHB* methylation was correlated with *MYCN* amplification in tumors of infants and children, but *DCR2* methylation was not (Table 2 and Fig. 2). Based on classification by the ploidy status, the association between *RASSF1A* or *PCDHB* methylation and *MYCN* amplification was observed in diploid tumors of infants and children; triploid tumors in infants had no *MYCN* amplification, therefore, associations could not be examined. *CASP8* methylation was associated with *MYCN* amplification in diploid tumors of infants and children, and triploid tumors in children.

Regarding to overall survival, the present study using conventional and/or quantitative MSP analysis exhibited association between *RASSF1A*, *DCR2*, and *PCDHB* methylation and poor outcomes in infants and children (Table 3 and Fig. 1), especially in diploid tumors of infants, and triploid tumors of children; *CASP8* methylation was only associated with a poor outcome in infants with a diploid tumor. Thus, *RASSF1A* methylation was associated with at a more advanced stage, *MYCN* amplification, and a poor outcome in infants with a diploid tumor. Although a substantial number of triploid tumors in infants exhibited *RASSF1A* methylation by conventional MSP analysis, they had no *MYCN* amplification and showed a favorable outcome, suggesting triploid tumors in infants as a specific biological subtype of neuroblastoma. Children with *RASSF1A*-, *DCR2*-, and *PCDHB*-methylated tumors had poorer outcomes than children with *RASSF1A*-, *DCR2*-, and *PCDHB*-unmethylated tumors, respectively. The association between *RASSF1A* and *DCR2* methylation and a poor outcome in children with triploid tumors is noteworthy, because the association was also observed in infants having a diploid tumor with or without *RASSF1A* and *DCR2* methylation. These findings suggest 2 subtypes of triploid neuroblastoma; while one was common in infants, exhibited hypomethylation of *RASSF1A* and *DCR2*, no *MYCN* amplification, and a favorable outcome, the other was common in children, exhibited hypermethylation of *RASSF1A*, *DCR2*, and *PCDHB*, frequent *MYCN* amplification, and an unfavorable outcome. We previously stated that triploidy in infant neuroblastoma may arisen through tetraploidization and succeeding tripolar division, whereas triploidy in childhood neuroblastoma may have derived from tetraploidization and chromosome loss [36]. We suggest that different mechanisms of triploid formation may have contributed to the different epigenetic features between infant and childhood triploid tumors. INRG proposed that patients with a hyperdiploid tumor be classified at low risk, whereas patients with a diploid tumor be classified at intermediate risk if they were $\leqslant$18 months of age and at the distantly metastatic stage [33]. We provided the data on epigenetic differences between diploid and triploid tumors in infants, and supported the inclusion of the ploidy status as one of factors included in the INRG classification system.

A recent study proposed a model in which the binding of TNFα to the death receptor, TNFαR1 results in its internalization, and subsequent formation of a complex with MOAP-1/RASSF1A to promote the open form of MOAP-1 to associate with Bax. This in turn results in Bax conformational changes and recruitment to the mitochondria to initiate cell death [10]. Silencing of *RASSF1A* due to promoter methylation by DNMT3B facilitated by MYCN and PRC2 was shown to avoid neuroblastoma cells entering apoptosis [37]. Thus, we consider that *RASSF1A*-methylated diploid tumors avoid entering apoptosis, facilitate proliferation, and finally cause unfavorable outcomes in infants and children with overexpressed MYCN with or without *MYCN* amplification.

On the other hand, aneuploidy has been shown to cause a proliferative disadvantage in yeast because of the overexpression of certain metabolism-associated genes [38], and it has been speculated that hypermethylation of the promoter regions of genes in cancer cells may lessen the metabolic impact of aneuploidy by silencing genes on a supernumerary chromosome while preserving the expression of other genes on chromosome that confer a selective advantage [39]. We propose that *RASSF1A* methylation in triploid neuroblastomas in infants found by mass-screening or diagnosed clinically may modulate their expression levels to repress cell cycle arrest and microtubule stabilization.

DCR2 is an antiapoptotic decoy receptor, which disturbs TRAIL-induced apoptosis in normal cells [29]. The present findings showing that *MYCN* amplification was associated with *RASSF1A*, *CASP8*, and *PCDHB* methylation, but not with *DCR2* methylation, may be explained by the transcriptional regulation of MYCN to the *RASSF1A*, *CASP8*, and *PCDHB* promoters, but not to the *DCR2* promoter.

In conclusion, the present study disclosed 2 subtypes of triploid neurblastoma with different clinical and epigenetic characteristics. These findings will facilitate understanding of heterogeneous biology of neuroblastoma, and improve choice of the treatment.

Conflict of interest

None.

Appendix A. Supplementary material

Supplementary data associated with this article can be found, in the online version, at http://dx.doi.org/10.1016/j.canlet.2014.03.022.

References

[1] J.M. Maris, M.D. Hogarty, R. Bagatell, S.L. Cohn, Neuroblastoma, Lancet 369 (2007) 2106–2115.
[2] G.M. Brodeur, Neuroblastoma: biological insights into a clinical enigma, Nat. Rev. Cancer 3 (2003) 203–216.
[3] M. Schwab, F. Westermann, B. Hero, F. Berthold, Neuroblastoma: biology and molecular and chromosomal pathology, Lancet Oncol. 4 (2003) 472–480.
[4] T. Sawada, M. Hirayama, T. Nakata, T. Takeda, N. Takasugi, T. Mori, et al., Mass screening for neuroblastoma in infants in Japan, Lancet 2 (1984) 271–273.
[5] W.G. Wood, R.N. Gao, J.J. Shuster, L.L. Robison, M. Bernstin, S. Weitzman, et al., Screening of infants and mortality due to neuroblastoma, N. Engl. J. Med. 346 (2002) 1041–1046.
[6] F.H. Schilling, C. Spix, F. Berthold, R. Erttmann, N. Fehse, B. Hero, et al., Neuroblastoma screening at one year of age, N. Engl. J. Med. 346 (2002) 1047–1053.
[7] E. Hiyama, T. Iehara, T. Sugimoto, M. Fukuzawa, Y. Hayashi, F. Sasaki, et al., Effectiveness of screening for neuroblastoma at 6 months of age: a retrospective population-based cohort study, Lancet 371 (2008) 1173–1180.
[8] A. Agathanggelou, W.N. Cooper, F. Latif, Role of the Ras-association domain family 1 tumor suppressor gene in human cancer, Cancer Res. 65 (2005) 3497–3508.
[9] A.M. Richter, G.P. Pfeifer, R.H. Dammann, The RASSF proteins in cancer; from epigenetic silencing to functional characterization, Biochim. Biophys. Acta 1796 (2009) 114–128.

Please cite this article in press as: M. Haruta et al., *RASSF1A* methylation may have two biological roles in neuroblastoma tumorigenesis depending on the ploidy status and age of patients, Cancer Lett. (2014), http://dx.doi.org/10.1016/j.canlet.2014.03.022

[10] M. Gordon, S. Baksh, RASSF1A: not a prototypical Ras effector, Small GTPases 2 (2011) 148–157.
[11] S. Honda, M. Haruta, W. Sugawara, F. Sasaki, M. Ohira, T. Matsunaga, et al., The methylation status of *RASSF1A* promoter predicts responsiveness to chemotherapy and eventual cure in hepatoblastoma patients, Int. J. Cancer 123 (2008) 1117–1125.
[12] J. Wang, B. Wang, X. Chen, J. Bi, The prognostic value of RASSF1A promoter hypermethylation in non-small cell lung carcinoma: a systematic review and meta-analysis, Carcinogenesis 32 (2011) 441–446.J.
[13] J. Ohshima, M. Haruta, Y. Fujiwara, N. Watanabe, Y. Arai, T. Ariga, et al., Methylation of the *RASSF1A* promoter is predictive of poor outcome among patients with Wilms tumor, Ped. Blood Cancer 59 (2012) 499–505.
[14] D. Astuti, A. Agathanggelou, S. Honorio, A. Dallol, T. Martinsson, P. Kogner, et al., *RASSF1A* promoter region CpG island hypermethylation in phaeochromocytomas and neuroblastoma tumours, Oncogene 20 (2001) 7573–7577.
[15] Q. Yang, P. Zage, D. Kagan, Y. Tian, R. Seshadri, H.R. Salwen, et al., Association of epigenetic inactivation of *RASSF1A* with poor outcome in human neuroblastoma, Clin. Cancer Res. 10 (2004) 8493–8500.
[16] B. Banelli, I. Gelvi, A. Di Vinci, P. Scaruffi, I. Casciano, G. Allemanni, et al., Distinct CpG methylation profiles characterize different clinical groups of neuroblastic tumors, Oncogene 24 (2005) 5619–5628.
[17] P. Lázcoz, J. Muñoz, M. Nistal, A. Pestaña, I. Encío, J.S. Castresana, Frequent promoter hypermethylation of RASSF1A and CASP8 in neuroblastoma, BMC Cancer 6 (2006) 254–264.
[18] Q. Yang, C.M. Kiernan, Y. Tian, H.R. Salwen, A. Chlenski, B.A. Brumback, et al., Methylation of *CASP8*, *DCR2*, and *HIN-1* in neuroblastoma is associated with poor outcome, Clin. Cancer Res. 13 (2007) 3191–3197.
[19] M.B. Michalowski, F. Fraipont, D. Plantaz, S. Michelland, V. Combaret, M.C. Favrot, Methylation of tumor-suppressor genes in neuroblastoma: the RASSF1A gene is almost always methylated in primary tumors, Ped. Blood Cancer 50 (2008) 29–32.
[20] A. Misawa, S. Tanaka, S. Yagyu, K. Tsuchiya, T. Iehara, T. Sugimoto, et al., *RASSF1A* hypermethylation in pretreatment serum DNA of neuroblastoma patients: a prognostic marker, Br. J. Cancer 100 (2009) 399–404.
[21] J. Hoebeeck, E. Michels, F. Pattyn, V. Combaret, J. Vermeulen, N. Yigit, et al., Aberrant methylation of candidate tumor suppressor genes in neuroblastoma, Cancer Lett. 273 (2009) 336–346.
[22] E. Grau, F. Martinez, C. Orellana, A. Canete, Y. Yañez, S. Oltra, et al., Hypermethylation of apoptotic genes as independent prognostic factor in neuroblastoma disease, Mol Carcinog. 50 (2011) 153–162.
[23] J. Stutterheim, F.A. Ichou, E. Ouden, R. Versteeg, H.N. Caron, G.A. Tytgat, et al., Methylated RASSF1a is the first specific DNA marker for minimal residual disease testing in neuroblastoma, Clin. Cancer Res. 18 (2012) 808–814.
[24] N.B. Kiss, P. Kogner, J.I. Johnsen, T. Martinsson, C. Larsson, J. Geli, Quantitative global and gene-specific promoter methylation in relation to biological properties of neuroblastomas, BMC Med. Genet. (2012), http://dx.doi.org/10.1186/1471-2350-13-83.
[25] T. Teitz, T. Wei, M.B. Valentine, E.F. Vanin, J. Grenet, V.A. Valentine, et al., Caspase 8 is deleted or silenced preferentially in childhood neuroblastomas with amplification of *MYCN*, Nat. Med. 6 (2000) 529–535.
[26] J. Takita, H.W. Yang, Y.Y. Chen, R. Hanada, K. Yamamoto, T. Teitz, et al., Allelic imbalance on chromosome 2q and alterations of the caspase 8 gene in neuroblastoma, Oncogene 20 (2001) 4424–4432.
[27] P. Gonzalez-Gomez, M.J. Bello, J. Lomas, D. Arjona, M.E. Alonso, C. Amiñoso, et al., Aberrant methylation of multiple genes in neuroblastic tumours: relationship with *MYCN* amplification and allelic status at 1p, Eur. J. Cancer 39 (2003) 1478–1485.
[28] K. Asada, N. Watanabe, Y. Nakamura, M. Ohira, F. Westermann, M. Schwab, A. Nakagawara, T. Ushijima, Stronger prognostic power of the CpG island methylator phenotype than methylation of individual genes in neuroblastomas, Jpn. J. Clin. Oncol. 43 (2013) 641–645.
[29] M.M. van Noesel, S. Bezouw, G.S. Salomons, P.A. Voûte, R. Pieters, S.B. Baylin, et al., Tumor-specific down-regulation of the tumor necrosis factor-related apoptosis-inducing ligand decoy receptors DcR1 and DcR2 is associated with dense promoter hypermethylation, Cancer Res. 62 (2002) 2157–2161.
[30] S. Yagyu, T. Gotoh, T. Iehara, M. Miyachi, Y. Katsumi, S. Tsubai-Shimizu, et al., Circulating methylated-*DCR2* gene in serum as an indicator of prognosis and therapeutic efficacy in patients with *MYCN* nonamplified neuroblastoma, Clin. Cancer Res. 14 (2008) 7011–7019.
[31] M. Abe, M. Ohira, A. Kaneda, Y. Yagi, S. Yamamoto, Y. Kitano, T. Takato, A. Nakagawara, T. Ushijima, CpG island methylator phenotype is a strong determinant of poor prognosis in neuroblastomas, Cancer Res. 65 (2005) 828–834.
[32] Y. Kaneko, H. Kobayashi, N. Watanabe, N. Tomioka, A. Nakagawara, Biology of neuroblastomas that were found by mass screening at 6 months of age in Japan, Ped. Blood Cancer 46 (2006) 285–291.
[33] S.L. Cohn, A.D. Pearson, W.B. London, T. Monclair, P.F. Ambros, G.M. Brodeur, et al., The International Neuroblastoma Risk Group (INRG) classification system: an INRG task force report, J. Clin. Oncol. 27 (2009) 289–297.
[34] Y. Kaneko, H. Kobayashi, N. Maseki, A. Nakagawara, M. Sakurai, Disomy 1 with terminal 1p deletion was frequent in mass screening-negative/late-presenting neuroblastomas in young children, but not in mass screening-positive neuroblastomas in infants, Int. J. Cancer 80 (1999) 54–59.
[35] J.G. Herman, J.R. Graff, S. Myöhänen, B.D. Nelkin, S.B. Baylin, Methylation-specific PCR: a novel PCR assay for methylation status of CpG islands, Proc. Natl. Acad. Sci. USA 93 (1996) 9821–9826.
[36] Y. Kaneko, A.G. Knudson, Mechanism and relevance of ploidy in neuroblastoma, Genes Chromosomes Cancer 29 (2000) 89–95.
[37] R.K. Palakurthy, N. Wajapeyee, M.K. Santra, C. Gazin, L. Lin, S. Gobeil, et al., Epigenetic silencing of the *RASSF1A* tumor suppressor gene through HOXB3-mediated induction of *DNMT3B* expression, Mol. Cell 36 (2009) 219–230.
[38] T. Galitski, A.J. Saldanha, C.A. Styles, E.S. Lander, G.R. Fink, Ploidy regulation of gene expression, Science 285 (1999) 251–254.
[39] P.V. Jallepalli, D. Pellman, Cell biology. Aneuploidy in the balance, Science 317 (2007) 904–905.

Please cite this article in press as: M. Haruta et al., *RASSF1A* methylation may have two biological roles in neuroblastoma tumorigenesis depending on the ploidy status and age of patients, Cancer Lett. (2014), http://dx.doi.org/10.1016/j.canlet.2014.03.022

European Journal of Cancer (2014) 50, 1555–1565

Available at www.sciencedirect.com

ScienceDirect

journal homepage: www.ejcancer.com

Novel 1p tumour suppressor Dnmt1-associated protein 1 regulates MYCN/ataxia telangiectasia mutated/p53 pathway

Yohko Yamaguchi [a], Hisanori Takenobu [a], Miki Ohira [b], Atsuko Nakazawa [c], Sayaka Yoshida [a], Nobuhiro Akita [a], Osamu Shimozato [a], Atsushi Iwama [d], Akira Nakagawara [e], Takehiko Kamijo [a,*]

[a] *Division of Biochemistry and Molecular Carcinogenesis, Chiba Cancer Center Research Institute, Japan*
[b] *Laboratory of Cancer Genomics, Chiba Cancer Center Research Institute, Japan*
[c] *Department of Pathology, National Center for Child Health and Development, Japan*
[d] *Department of Cellular and Molecular Medicine, Graduate School of Medicine, Chiba University, Chiba, Japan*
[e] *Division of Biochemistry and Innovative Cancer Therapeutics, Chiba Cancer Center Research Institute, Japan*

Available online 19 February 2014

KEYWORDS
DMAP1
ATM
p53
Neuroblastoma
MYCN

Abstract Neuroblastoma (NB) is a paediatric solid tumour which originates from sympathetic nervous tissues. Deletions in chromosome 1p are frequently found in unfavourable NBs and are correlated with v-myc avian myelocytomatosis viral oncogene neuroblastoma derived homolog (*MYCN*) amplification; however, it remains to be elucidated how the 1p loss contributes to MYCN-related oncogenic processes in NB. In this study, we identified the role of Dnmt1-associated protein 1 (DMAP1), coded on chromosome 1p34, in the processes.
We studied the expression and function of DMAP1 in NB and found that low-level expression of DMAP1 related to poor prognosis, unfavourable histology and 1p Loss of heterozygosity (LOH) of primary NB samples. Intriguingly, DMAP1 induced ataxia telangiectasia mutated (ATM) phosphorylation and focus formation in the presence of a DNA damage reagent, doxorubicin. By DMAP1 expression in NB and fibroblasts, p53 was activated in an ATM-dependent manner and p53-downstream pro-apoptotic Bcl-2 family molecules were induced at the mRNA level, resulting in p53-induced apoptotic death. *BAX* and $p21^{Cip1/Waf1}$ promoter activity dependent on p53 was clearly up-regulated by DMAP1. Further, MYCN transduction in *MYCN* single-copy NB cells accelerated doxorubicin (Doxo)-induced apoptotic cell death; MYCN is implicated in DMAP1 protein stabilisation and ATM phosphorylation in these situations. DMAP1 knockdown attenuated MYCN-dependent ATM phosphorylation and NB cell apoptosis. Together, DMAP1

* *Corresponding author:* Address: Division of Biochemistry and Molecular Carcinogenesis, Chiba Cancer Center Research Institute, 666-2 Nitona, Chuo-ku, Chiba 260-8717, Japan. Tel.: +81 43 264 5431; fax: +81 43 265 4459.
E-mail address: tkamijo@chiba-cc.jp (T. Kamijo).

http://dx.doi.org/10.1016/j.ejca.2014.01.023

appears to be a new candidate for a 1p tumour suppressor and its reduction contributes to NB tumourigenesis via inhibition of MYCN-related ATM/p53 pathway activation.

1. Introduction

Genetic and molecular analyses have indicated various types of deletions of the short arm of chromosome 1 (1p) in a broad range of human malignant tumours, including neuroblastoma (NB) and others [1–5]. It has been suggested that this genomic region harbours several tumour suppressor genes and that additive effects of loss of those tumour suppressors on tumourigenesis exist in several '1p loss malignant tumours'.

NB is the second most common paediatric solid malignant tumour derived from sympathetic nervous tissues. Extensive cytogenetic and molecular genetic studies have identified that genetic abnormalities, such as loss of the short arm of 1p, 11q and 14q; amplification of *MYCN*; and allelic gain of 11p and 17q, are frequently observed [1]. Deletion of the 1p region is highly correlated with both *MYCN* amplification and an adverse patient outcome, indicating the presence of several tumour suppressor genes (TSGs) within this region [6]. NB tumours with *MYCN* in a single copy had preferentially lost the 1p36 allele and these tumours also had a very distal commonly deleted region; in contrast, all *MYCN*-amplified NBs had larger 1p deletions, extending from the telomere to 1p31 [7]. The extent of deletion or LOH was identified in 184 primary NBs; in 80%, the 1p deletion extended from the telomere to 1p31 [8]. Given the tendency of large, hemizygous 1p deletions in *MYCN*-amplified NBs, alternative hypotheses for tumour suppression are: (1) an additional, *MYCN*-associated TSG in the 1p region; (2) suppression of TSG expression from a hemizygous allele due to epigenetic modifications except for imprinting, e.g. miRNAs and non-coding RNAs; (3) haplo-insufficiency-based suppression accounting for the rarity of 1p homozygous deletions [9].

Dnmt1-associated protein 1 (DMAP1) was originally identified as a molecule interacting with DNMT1 and was demonstrated to co-localise with PCNA and DNMT1 at DNA replication foci during the S phase [10]. Previously, we reported that Dmap1 participates in DNA repair and transformation of mouse embryonic fibroblasts (MEFs). Dmap1 was recruited to the damaged sites, formed complexes with γ-H2AX and directly interacted with Proliferating Cell Nuclear Antigen (Pcna); inhibition of this binding impaired the accumulation of the Pcna-Caf-1 complex at damaged sites and resulted in DNA breaks [11]. In addition, Penicud and Behrens reported that DMAP1 promotes ataxia telangiectasia mutated (ATM) recruitment and focus formation at damaged sites. These results suggest that DMAP1 is involved in the DNA damage response (DDR) [12]. Interestingly, DMAP1 gene is coded in 1p34 and the region that is frequently deleted in NB tumours with 1p LOH [8,9]. These results prompted us to study the expression level of DMAP1 in neuroblastoma samples and its functional role in tumourigenesis.

In the present report, for the first time, we found that DMAP1 is a novel 1p tumour suppressor and DMAP1 has an indispensable role in MYCN-related ATM/p53 pathway activation. Downregulation of DMAP1 seems to be a result of MYCN-induced stress and an important mechanism for NB tumourigenesis.

2. Materials and methods

2.1. Cell culture

Human NB cell lines were obtained from official cell banks (RIKEN Bioresource Cell Bank, Tohoku University Cell Resource Center, and the American Type Culture Collection) and were cultured in RPMI1640 or Dulbecco's modified Eagle's medium (Wako, Osaka, Japan) supplemented with 10% heat-inactivated foetal bovine serum (Invitrogen, Carlsbad, CA, United States of America (USA)) and 50 μg/ml penicillin/streptomycin (Sigma–Aldrich, St. Louis, MO, USA) in an incubator with humidified air at 37 °C with 5% CO_2. ATM kinase inhibitor, KU-55933 (Santa Cruz Biotechnology, Santa Cruz, CA, USA) was dissolved in DMSO to make stock solutions of 20 mM.

2.2. Lentiviral production and infection for over-expression and knockdown of genes

For the over-expression of mouse Dmap1 and human DMAP1, cDNAs were subcloned into lentiviral vector pHR-SIN-CSGW [13]. For shRNA-based knockdown experiments, pLKO.1 puromycin-based lentiviral vectors containing five sequence-verified shRNAs targeting human DMAP1 (RefSeq NM_019100.4, NM_001034024.1, NM_001034023.1) were obtained from the MISSION TRC-Hs 1.0 Human, shRNA library (Sigma–Aldrich). We checked DMAP1 knockdown by five lentivirus-produced shRNAs (clones: TRCN0000021744-21748) and used at least two shRNAs for experiments. Lentiviral production, infection and confirmation of infection efficiency were performed as described previously [13].

2.3. Antibodies

Antibodies against p53 (DO-1) and MYCN (rabbit polyclonal, C-19) were purchased from Santa Cruz Biotechnology. Antibodies against p53Ser15-P (rabbit

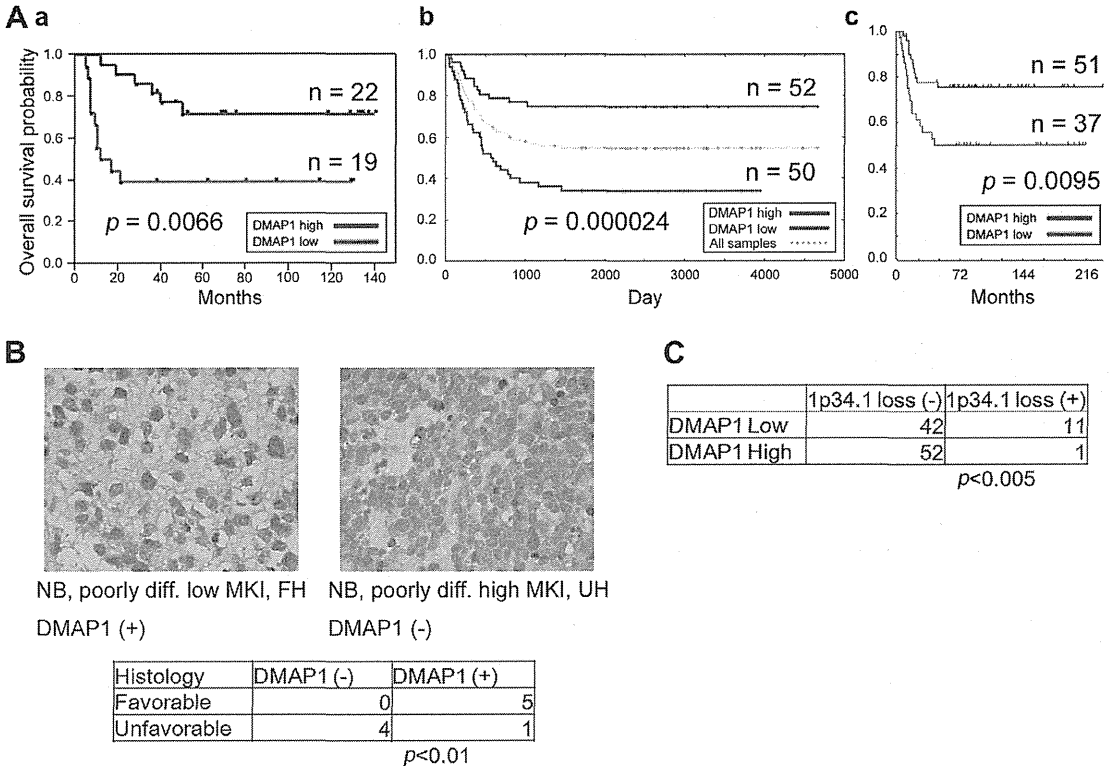

Histology	DMAP1 (-)	DMAP1 (+)
Favorable	0	5
Unfavorable	4	1

$p<0.01$

	1p34.1 loss (-)	1p34.1 loss (+)
DMAP1 Low	42	11
DMAP1 High	52	1

$p<0.005$

Fig. 1. Expression level of Dnmt1-associated protein 1 (DMAP1) in neuroblastoma (NB) samples and neuroblastoma cell lines. (A) Kaplan–Meier survival analysis of NB patients based on higher or lower expression levels of *DAMP1* (overall survival analysis) presented by microarray analysis in three individual cohorts. (Aa) Chiba Cancer Center Research Institute cohort ($n = 41$). Expression levels of *DMAP1* were separated into a high or low group based on the average expression. Statistical analysis was performed by the log-rank test. Corresponding p values are indicated. (Ab) Childrens Hospital Los Angeles cohort (http://pob.abcc.ncifcrf.gov/cgi-bin/JK), Neuroblastoma Prognosis Database-Seeger Lab dataset. $n = 102$. Expression levels of *DMAP1* on probe 224163_s_at were separated into a high or low group based on the median expression. (Ac) Academic Medical Center cohort R2 microarray analysis and visualisation platform (http://r2.amc.nl), Tumor Neuroblastoma public-Versteeg-88 dataset. $n = 88$. Expression levels of *DMAP1* on probe 224163_s_at were separated into a high or low group based on the expression cutoff value 118.0 according to the R2 algorithm. (B) Immunohistochemical staining for DMAP1 in NB. Statistical significance was determined by Fisher's exact probability test. MKI: Mitosis-karyorrhexis index. FH: favourable histology; UH: unfavourable histology. DMAP1 (+): DMAP1 high-expression tumour; DMAP1 (−): DMAP1 low-expression tumour. (C) 1p loss was studied by array CGH analysis. Expression status of *DMAP1* was quantified by quantitative polymerase chain reaction (qPCR) analysis and normalised by *GAPDH* expression. *DMAP1* high or low expression was determined by its median value. Fisher's exact probability test was applied to determine statistical significance.

polyclonal) and ATMSer1981-P (10H11. E12) were from Cell Signaling Technology (Danvers, MA, USA). Anti-ATM rabbit polyclonal antibody (Ab-3) was from Merck Millipore. Antibodies against β-Actin (rabbit polyclonal) and anti-FLAG (M2) were from Sigma–Aldrich. A mouse monoclonal anti-tubulin antibody was from Neomarkers Lab Vision (Fremont, CA, USA). Anti-DMAP1 rabbit polyclonal antibody (ab2848) was from Abcam (Cambridge, United Kingdom (UK)), anti-DMAP1 (2G12) was from Abnova (Taipei, Taiwan) and anti-human influenza hemagglutinin (HA) rabbit polyclonal was from MBL (Nagoya, Japan).

2.4. Statistical analysis

All data were tested statistically using the Welch test and Fisher's exact probability test. $p < 0.05$ was considered to indicate statistical significance. Kaplan–Meier survival curves were calculated, and survival distributions were compared using the log-rank test. Cox regression models were used to explore associations between *DMAP1* expression, age at diagnosis, tumour stage, *TrkA* expression, *MYCN* copy number, tumour origin, DNA ploidy, Shimada pathology and survival. Statistical significance was declared if $p < 0.05$. Statistical analysis was performed using JMP 8.0 (SAS Institute Inc., Cary, NC, USA).

Other methods are described in Supplementary information.

3. Results

3.1. Low expression level of DMAP1 correlated with unfavourable prognosis of NB patients

We examined the expression levels of *DMAP1* in NB samples by microarray analysis. Kaplan–Meier survival analysis showed that low *DMAP1* expression correlated

with the unfavourable prognosis of NB patients (Fig. 1Aa). Web-based microarray analysis and visualisation application for NB confirmed these results (Fig. 1Ab, c), and it was also shown by quantitative polymerase chain reaction (qPCR) (Suppl. Fig. S1Aa). Unfavourable NBs, which are classified by International Neuroblastoma Staging System (INSS) stage with *MYCN* copy number, also expressed low-level *DMAP1* (Suppl. Fig. S1B). Immunohistochemical analysis also showed low expression of *DMAP1* in unfavourable histology NB (Fig. 1B).

Next, the chromosome 1p status was analysed by array CGH to study the mechanism of *DMAP1* reduction in unfavourable NB (Fig. 1C). As a result, *DMAP1* reduction in unfavourable NB was significantly correlated with loss of its gene locus. DMAP1 mRNA levels were significantly lower in NB cell lines than in primary NB samples (Suppl. Fig. S1C). To further assess other possibilities for the suppression of *DMAP1* expression, bisulphite sequencing was carried out using five clinical samples and two cell lines of NB and *BMI1* knockdown to study epigenetic suppression by polycombs in NB cell lines; however, DNA methylation of the *DMAP1* promoter region and transcriptional suppression of *DMAP1* by *BMI1* were not found (data not shown). Next, univariate Cox regression was employed to examine the individual relationship of each variable to survival (Table 1). These variables were: *DMAP1* expression, age at diagnosis (>1 year old versus <1 year old), tumour stage (3 + 4 versus 1 + 2 + 4s), *TrkA* expression (low versus high), *MYCN* copy number (amplified versus non-amplified), origin (adrenal gland versus others), DNA ploidy (aneuploidy versus di-/tetraploidy) and Shimada pathology (favourable versus unfavourable), all of which were found statistically to be of prognostic importance. Additionally, multivariable Cox analysis demonstrated that *DMAP1* expression was an independent prognostic factor from tumour origin, stage and DNA ploidy. However, the analysis showed a correlation between *DMAP1* reduction and *MYCN* amplification (Table 1). These results suggested that *DMAP1* works as a tumour suppressor gene in NB and its expression levels strongly correlate with *MYCN* copy numbers.

Table 1
Correlation between Dnmt1-associated protein 1 (DMAP1) expression and other prognostic factors of neuroblastoma.

Terms	High DMAP1	Low DMAP1	*p*-Value
Age (years)			
≤1.5	25	33	0.13
>1.5	31	23	
Tumour origin			
Adrenal	29	28	0.773
Others	26	28	
Stage			
1, 2, 4S	29	22	0.184
3, 4	27	34	
Shimada pathology			
Favourable	37	30	0.16
Unfavourable	12	18	
MYCN copy number			
Single	52	41	<0.01
Amplified	4	15	
TrkA expression			
High	32	28	0.507
Low	23	26	
DNA index			
Diploidy	22	27	0.186
Aneuploidy	28	20	

MYCN: Fisher's exact probability test, $\chi^2 = 7.669496321$, $p < 0.01$.

3.2. DMAP1 activated ATM and p53 with DNA damage

In our previous study, we observed that Dmap1 knockdown in MEFs leads to the failure of DNA repair, resulting in accumulated DNA damage [11]. These results prompted us to study the role of DMAP1 in DDR, including the ATM/p53 pathway. In response to DNA damage, ATM forms foci at double-stranded DNA break (DSB) sites and undergoes self-phosphorylation at serine 1981 to enhance its kinase activity. The activated ATM phosphorylates p53 at serine 15, which in turn induces p53-downstream effectors, leading to the inhibition of cell cycle progression or apoptotic cell death [14]. For DNA damage induction, we chose doxorubicin (Doxo) at 0.5 μg/ml concentration to assess the effect on NB cells according to the results of the analysis of peak plasma concentrations of doxorubicin [15].

We expressed DMAP1 in p53-wild type NB cells and found that ATMSer1981 phosphorylation increased for up to 6 h after Doxo treatment, and p53Ser15 phosphorylation was up-regulated subsequently (Fig. 2A). We also confirmed DMAP1-related p53Ser15 phosphorylation in human fibroblasts (Fig. 2B).

Next, SH-SY5Y cells, which express rather higher DMAP1 than other NB cell lines (Suppl. Fig. S1D), were infected with shDMAP1-expressing virus and treated with Doxo. Knockdown of DMAP1 resulted in downregulation of ATM and p53 phosphorylation (Fig. 2C). We then evaluated the focus formation of ATM. It was significantly suppressed 1.0 h but not 1.5–2.5 h after Doxo treatment by DMAP1 knockdown (Fig. 2D), suggesting that DMAP1 is required for efficient focus formation of ATM in the early stage of DDR.

3.3. DMAP1 activated p53 by ATM and induced transcription of p53-downstream genes

To examine whether p53 phosphorylation promoted by DMAP1 is dependent on ATM activity, we used an

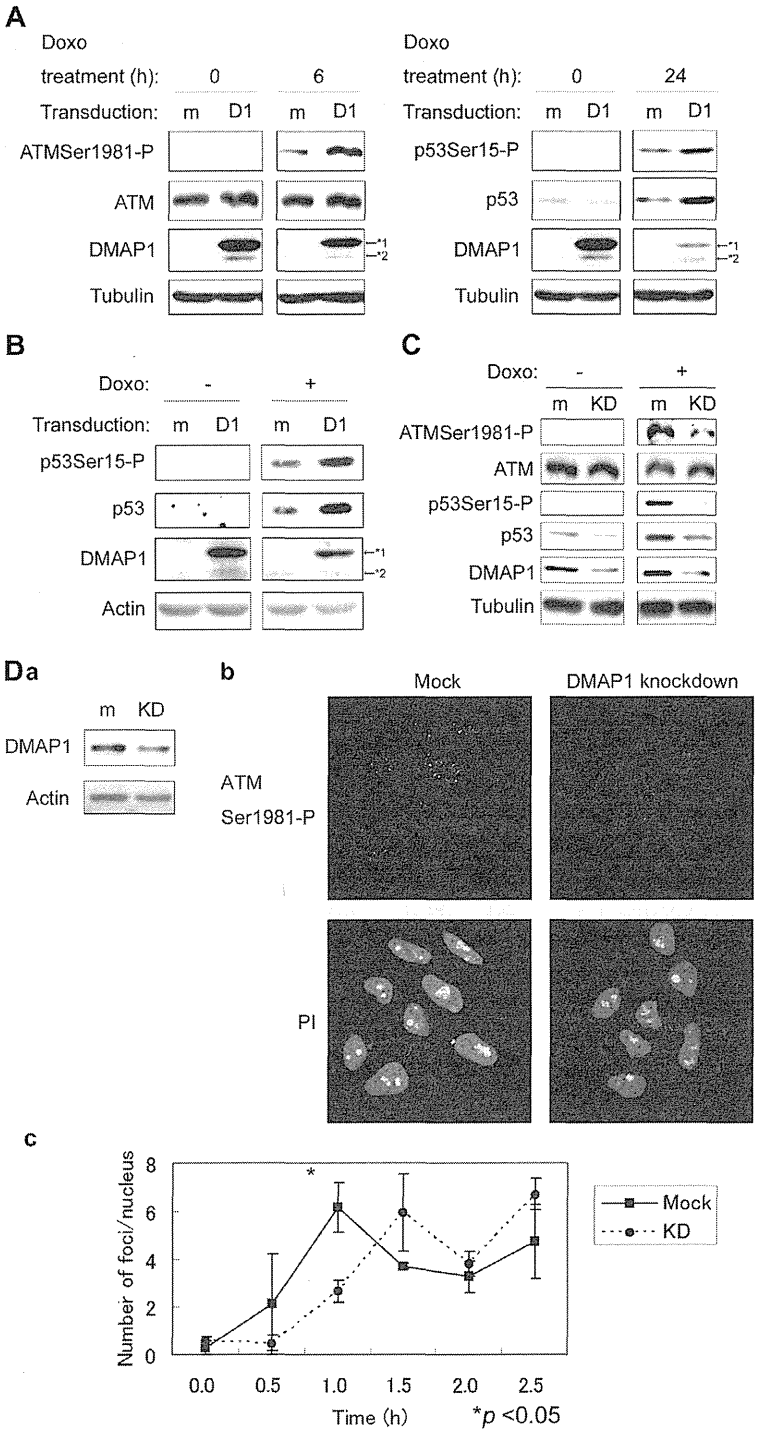

Fig. 2. Dnmt1-associated protein 1 (DMAP1) promoted focus formation of ataxia telangiectasia mutated (ATM) and activated ATM under doxorubicin (Doxo) treatment. (A) Phosphorylation status of ATMSer1981 and p53Ser15 in DMAP1 over-expressing cells. SK-N-SH cells were transduced with human influenza hemagglutinin (HA)-tagged DMAP1 and treated with Doxo for the indicated time period. The cells were subjected to sodium dodecyl sulphate–polyacrylamide gel electrophoresis (SDS–PAGE) and Western blot analysis. (B) Phosphorylation of p53Ser15 by DMAP1 in human fibroblasts (hfb). Hfb were transduced with HA-tagged DMAP1 and treated with Doxo for 24 h to confirm phosphorylation of p53 by Western blot analysis. (C) Phosphorylation status of ATMSer1981 in DMAP1 knocked-down cells. SH-SY5Y cells were infected with shDMAP1-expressing virus and treated with Doxo for 1 h. The cells were subjected to SDS–PAGE and Western blot analysis. (D) Focus formation of ATM in DMAP1 knocked-down cells. SH-SY5Y cells were infected with shDMAP1-expressing virus and treated with Doxo for the indicated time period, followed by SDS–PAGE, Western blot analysis (Da) and immunocytochemistry (ICC, Db). In ICC, cells were stained with anti-ATMSer1981-P and propidium iodide (PI). (Dc) Number of ATM foci was counted using the colony counting tool in Image Quant TL. Error bars represent S.D. obtained from triplicate samples. Data were analysed using the Welch test. Data are representative of three independent experiments. (A–D), m: mock, D1: DMAP1, KD: DMAP1 knockdown; *1: HA-DMAP1, *2: Endogenous DMAP1.

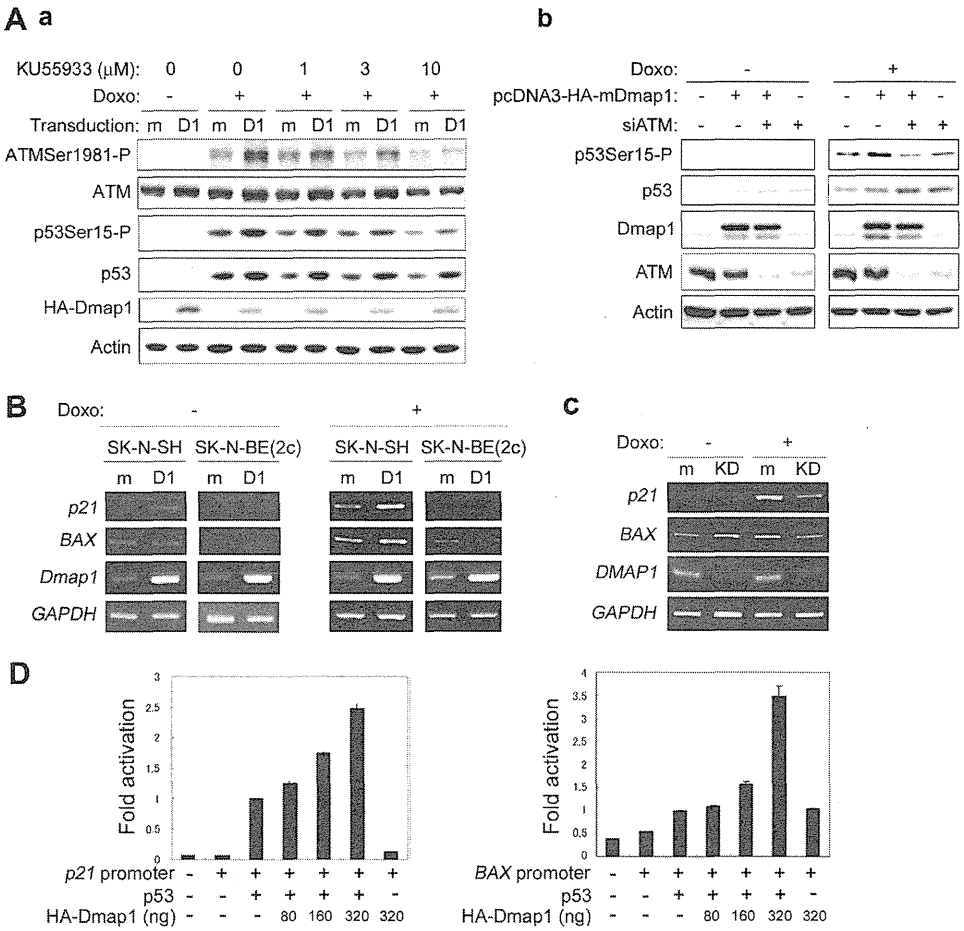

Fig. 3. Dnmt1-associated protein 1 (DMAP1) activated p53 via ataxia telangiectasia mutated (ATM). (A) Phosphorylation of p53Ser15 by Dmap1 thorough ATM activation. (Aa) SK-N-SH cells were infected with HA-tagged Dmap1-expressing virus and pre-treated with KU-55933. One hour after KU-55933 addition, cells were treated with doxorubicin (Doxo) for 12 h and subjected to sodium dodecyl sulphate–polyacrylamide gel electrophoresis (SDS–PAGE) and Western blot analysis. (Ab) SK-N-SH cells were transfected with *ATM* siRNA (sequence: 5′-AACATACTACTCAAAGACATT-3′, Sigma–Aldrich, St. Louis, MO, USA). or control siRNA (ON-TARGETplus Non-targeting siRNA #1, Thermo Fisher Scientific, Lafayette, CO, USA). Transfection of siRNA was performed according to a previous report (16). Forty-eight hours after forward transfection, the cells were treated with 0.3 μg/ml Doxo for 1 h and subjected to Western blot. m: mock, D1: Dmap1. (B, C) Semi-quantitative Reverse Transcription Polymerase Chain Reaction (RT-PCR) of p53-target genes in *Dmap1* over-expressing cells (B) and in DMAP1 knocked-down SH-SY5Y cells (C). m: mock, D1: Dmap1, KD: DMAP1 knockdown. (D) Luciferase reporter assay analysis of $p21^{Cip1/Waf1}$ and *BAX* promoter activity in H1299 cells. Increasing amount of pcDNA3-HA-Dmap1, constant amount of pcDNA 3-p53, Renilla luciferase reporter plasmid (pRL-TK) and luciferase reporter plasmid with p53 responsive elements were transfected, and luciferase activity was studied. Data are representative of three independent experiments ($n = 3$).

ATM-specific ATP-competitive inhibitor KU-55933. KU-55933 abrogated the Dmap1-induced phosphorylation of ATM and p53, indicating ATM dependency of Dmap1-related p53 phosphorylation (Fig. 3Aa). ATM knockdown further represented ATM-dependent p53Ser15 phosphorylation by DMAP1 (Fig. 3Ab). Downstream target genes of p53, such as $p21^{Cip1/Waf1}$ and *BAX*, were induced by Dmap1 in the presence or absence of Doxo in *p53*-wt SK-N-SH cells but were not induced in *p53*-mutated SK-N-BE(2c) cells (Fig. 3B). Knockdown of DMAP1 reduced p53 accumulation (Fig. 2C) and transcription of the downstream $p21^{Cip1/Waf1}$ and *BAX* in a Doxo-dependent manner (Fig. 3C). Transcription of *NOXA*, the pro-apoptotic Bcl-2 family molecule, which was previously shown to be a critical molecule in p53-related damage-induced NB cell death [16], was also upregulated by DMAP1 (Suppl. Fig. S2A). DMAP1-promoted upregulation of $p21^{Cip1/Waf1}$ and *BAX* promoter activity, which was mediated by p53, was confirmed by a luciferase reporter assay of *p53*-null H1299 cells (Fig. 3D).

3.4. DMAP1 acts as a tumour suppressor via p53 activation in NB cells

We examined the functional role of DMAP1 and its p53 dependency in NB cells. DMAP1 enhanced cell cycle arrest and apoptosis induced by Doxo in a

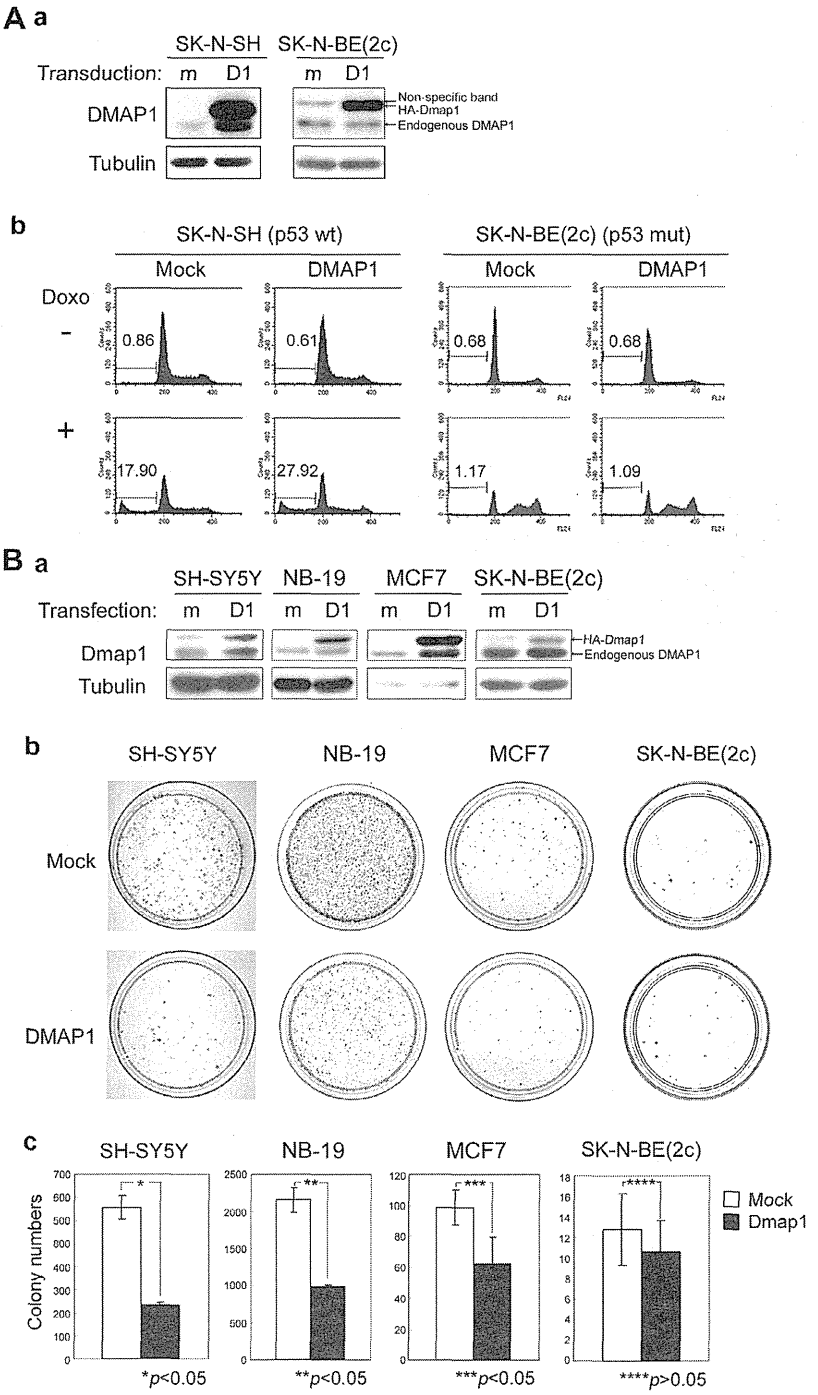

Fig. 4. Dnmt1-associated protein 1 (DMAP1) acts as a tumour suppressor via p53 activation in NB cells. (A) Dmap1-transduced NB cells were treated with doxorubicin (Doxo) and subjected to Western blot (Aa) and cell cycle analysis by flow cytometry (Ab). Numbers in histogram indicate % of subG0/G1 population. (B) Colony formation assay in Dmap1 over-expressing cells. Cells were transfected with pcDNA3-heteroduplex analysis (HA)-Dmap1 and subjected to Western blot (Ba) and selected with 400 μg/ml G418 for SH-SY5Y cells, 500 μg/ml G418 for NB-19 cells, 800 μg/ml G418 for MCF7 cells and 800 μg/ml G418 for SK-N-BE(2c) cells, for 2 weeks. (Bb) Colonies were stained with May-Grünwald's Eosin Methylene Blue Solution (Wako, Osaka, Japan) and Giemsa's solution (Merk Japan, Tokyo, Japan). (Bc) Number of colonies was counted using the colony counting tool in Image Quant TL. Error bars represent S.D. (A–B), m: mock, D1: Dmap1.

p53-dependent manner (Fig. 4A and Suppl. Fig. S2B). SH-SY5Y cells, NB-19 cells and breast cancer-derived MCF7 cells harbouring wild-type p53 were transfected with pcDNA3-HA-Dmap1 and selected with G418 for two weeks. As shown in Fig. 4B, Dmap1 significantly suppressed colony formation in these cells. These results suggested that DMAP1 acts as a tumour suppressor via p53 activation in NB cells.

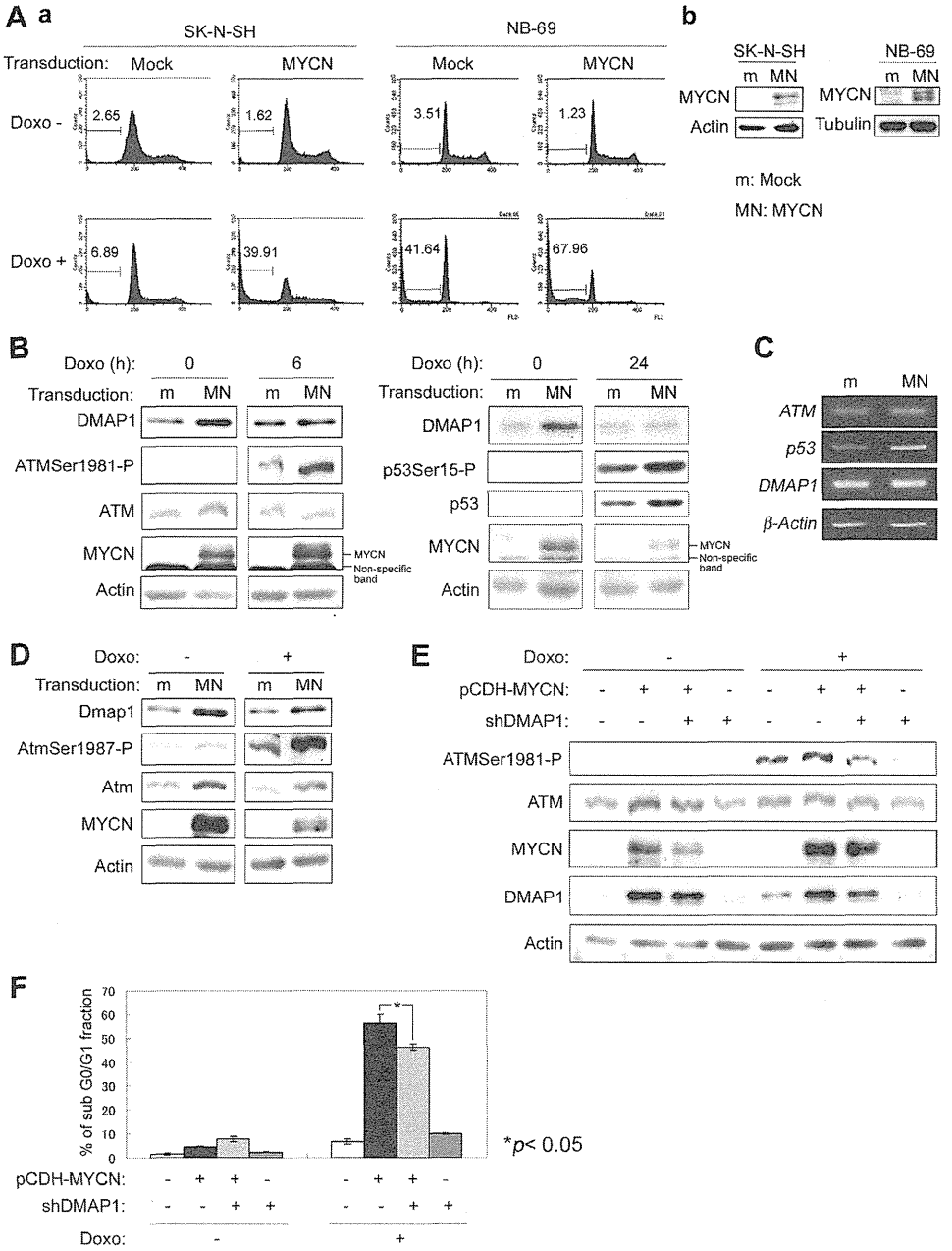

Fig. 5. MYCN promoted doxorubicin (Doxo)-induced apoptosis and ataxia telangiectasia mutated (ATM)/p53 activation. Cells were transduced with pCDH-MYCN and subjected to analysis as follows. (Aa) Cell cycle analysis [(Ab) protein expression was confirmed by Western blotting in left panel], (B) Western blot analysis and (C) semi-quantitative RT-PCR of MYCN over-expressing and Doxo-treated NB cells. Numbers in histogram indicate% of subG0/G1 population. (D) Activation of Atm/p53 pathway by MYCN in NIH3T3 cells. Cells were collected 12 h after Doxo treatment and subjected to Western blot analysis. (E, F) MYCN over-expression and/or Dnmt1-associated protein 1 (DMAP1) knockdown were performed as indicated in SK-N-SH cells. Cells were collected for Western blot analysis of ATMSer1981-P (E) and sub G0/G1 analysis (F) 6 h after Doxo treatment. (A–D) m: mock, MN: MYCN.

3.5. DMAP1 was implicated in MYCN-induced ATM activation

Given that *MYCN* amplification correlated with a low level of DMAP1 and that MYCN regulates the ATM/p53 pathway [17], we studied the DMAP1/ATM/p53 pathway in *MYCN*-transduced cells. As reported [18], exogenous MYCN promoted apoptosis in *MYCN* single-copy and *p53* wild type SK-N-SH cells and NB-69 cells (Fig. 5A) and activation of ATM/p53 under Doxo treatment in SK-N-SH cells (Fig. 5B left: 6 h after, right: 24 h after). Interestingly, the protein amount of DMAP1 was upregulated by MYCN although *DMAP1* mRNA was not increased (Fig. 5B, C).

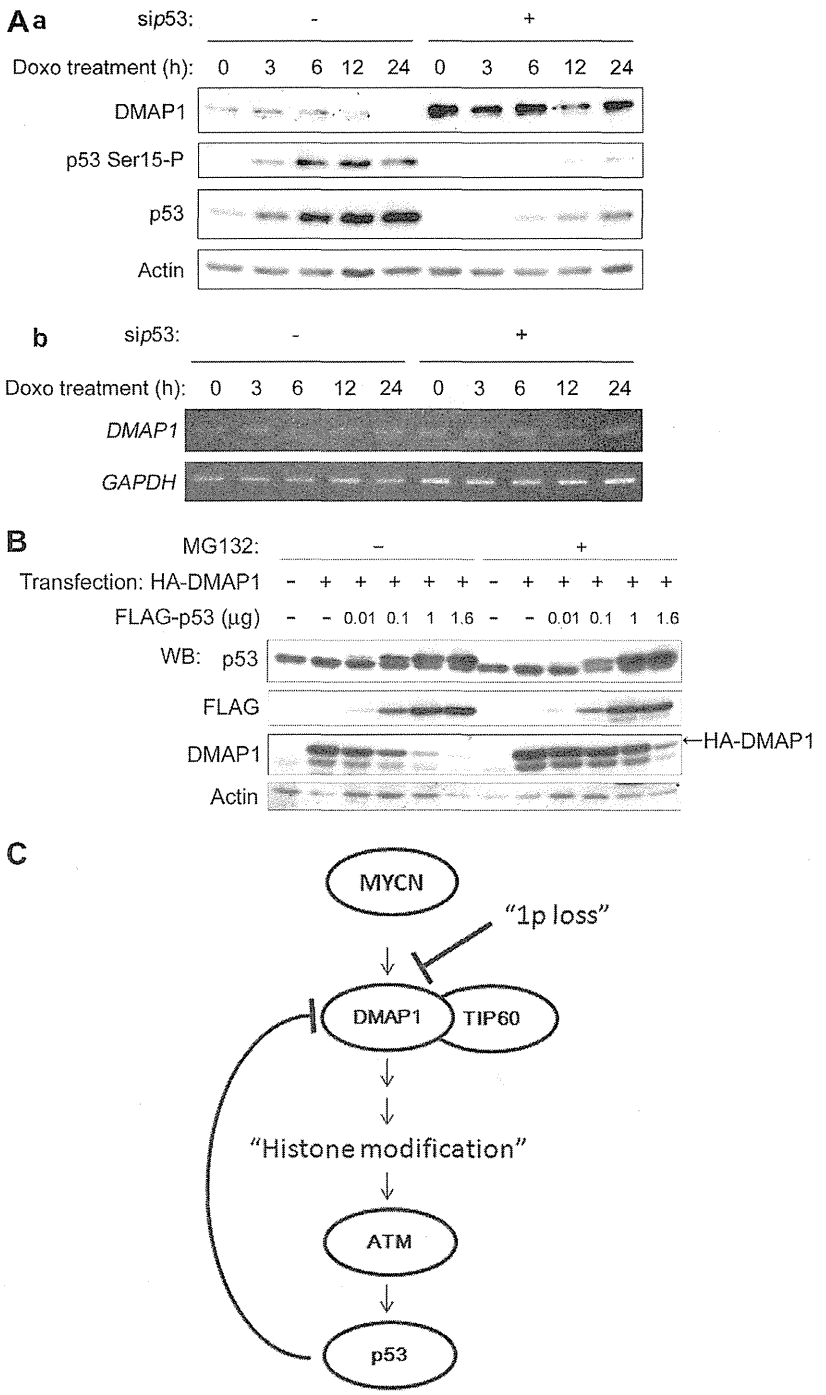

Fig. 6. Dnmt1-associated protein 1 (DMAP1) degradation by p53. (A) DMAP1 expression in p53 knocked-down cells. SK-N-SH cells harbouring wt-p53 were transfected with *p53* siRNA (ON-TARGETplus Duplex J-003329-14-0005, Human Tp53; Thermo Fisher Scientific, Lafayette, CO, USA) or control siRNA (Silencer_Negative Control #1 siRNA; Ambion Inc., Austin, TX, USA). Transfection of siRNA was performed according to a previous report (16). Forty-eight hours after forward transfection, the cells were treated with 0.3 μg/ml doxorubicin (Doxo) for the indicated time periods and subjected to Western blotting (Aa)/semi-quantitative RT-PCR (Ab). (B) Western blot analysis of Dmap1 degradation by p53 in combination with MG132 treatment. 293T cells were transfected with a constant amount of pcDNA3-heteroduplex analysis (HA)-tagged Dmap1 and increasing amounts of pcDNA3-FLAG-tagged p53 and then treated with 2 μM MG132 for 24 h. (C) MYCN/DMAP1/ataxia telangiectasia mutated (ATM)/p53 pathway regulates neuroblastoma cell death.

These phenomena were confirmed in *MYCN*-single copy, p53 wild-type NIH3T3 fibroblasts (Fig. 5D). Further, DMAP1 knockdown reduced the phosphorylation of ATM (Fig. 5E) and Doxo-induced apoptosis

(Fig. 5F), which were up-regulated by MYCN, indicating that DMAP1 was implicated in MYCN-induced ATM/p53 activation and apoptosis.

3.6. Negative feedback regulation of DMAP1 by p53

In MYCN-related ATM/p53 pathway activation, we found that DMAP1 protein was reduced, accompanied with p53 activation (Fig. 5B) and this DMAP1 reduction was also observed in DMAP1-tranduced cells after p53 activation by Doxo (Figs. 2A, B and 3A). To examine whether p53 reduces DMAP1, we knocked down p53 in NB cells (Fig. 6A). DMAP1 protein was clearly increased by p53 knockdown, but the mRNA level of DMAP1 was not affected. Proteasome inhibitor, MG132 treatment effectively inhibited DMAP1 degradation by p53 expression (Fig. 6B), suggesting that p53 promotes DMAP1 degradation in an ubiquitin–proteasome system-dependent manner.

4. Discussion

The proto-oncogenes *MYC* and *MYCN* have a pivotal function in growth control, differentiation and apoptosis and are among the most frequently affected genes in human malignant tumours; they are overexpressed in a large percentage of human tumours [19,20]. Transformation by Myc proteins requires concomitant inhibition of apoptosis by inactivation of apoptosis-inducing pathway genes [21]. One of the *MYC* oncogene product-related apoptotic pathways is involved in DDR [18]. Recent studies have clarified the relevant pathways regulating MYC-induced DDR, leading to the identification of ATM, TIP60 and WIP1 as mediators of this response [22]. Once ATM was activated by DNA damage, both p53 and proteins that interact with p53, MDM2 and Chk2 were phosphorylated by ATM, which in turn transactivated the p53-downstream effectors, leading to the inhibition of cell cycle progression or apoptotic cell death [23].

Regarding MYC/MYCN-related ATM regulation, this over-expression causes DNA damage *in vivo* and the ATM-dependent response to this damage is critical for p53 activation, apoptosis and the suppression of tumour development [22,24,25]. These findings suggested that MYC/MYCN expression induces ATM/p53 pathway activation by the related cellular stresses and subsequent inactivation of ATM will produce advantages for the tumourigenesis of MYC/MYCN-deregulated tumours. However, the occurrence of NB in ataxia-telangiectasia patients and ATM mutation in NB cells have not been reported to our knowledge, and mutations of p53 have been reported in <2% of NB [26,27], suggesting that functional inactivation of the pathway by other molecules seems to occur in NB tumours.

In the present study, we found that MYCN expression in *MYCN* single-copy cells increased DMAP1 and Doxo-induced apoptotic cell death (Fig. 5). DMAP1 induced ATMSer1981 phosphorylation and its focus formation in the presence of Doxo (Figs. 2 and 3A). By DMAP1 expression, p53Ser15 phosphorylation was induced in an ATM-dependent manner. In NB tumour samples, low expression of DMAP1 was related to poor prognosis, unfavourable histology, *MYCN* amplification and 1p LOH (Fig. 1, Table 1, Suppl. Fig. S1), suggesting that DMAP1 downregulation is required for NB tumourigenesis, especially under MYCN-induced cellular stress. Intriguingly, we observed negative feedback for degrading DMAP1, suggesting another DMAP1 downregulation mechanism in NB tumourigenesis (Fig. 6).

Recently, Penicud and Behrens reported that DMAP1 enhances Histone Acetyl Transferase (HAT) activity of TIP60 and promotes ATM auto-phosphorylation [12]. Depleting DMAP1 reduced ATM phosphorylation a few minutes after irradiation, but at later time points, it had no effect on ATM activation, as we previously reported [11]. Consistent with these observations, we found that DMAP1 knockdown delayed ATM focus formation and that the delay of ATM activation attenuated p53 phosphorylation and stabilisation. (Fig. 2C, D). These results indicate that DMAP1 regulates the efficient recruitment of ATM to the site of DNA breaks and this regulation is required for subsequent Doxo-induced p53-dependent cell death in NBs.

Taken together, we found that DMAP1 is a novel molecule of 1p tumour suppressors and has a role in ATM/p53 activation induced by MYCN-related cellular stresses (Fig. 6C). DMAP1 might be a new molecular target of MYCN-amplified NB treatment.

Conflict of interest statement

None declared.

Acknowledgements

We would like to thank Ms. Kumiko Sakurai and Dr. Masamitsu Negishi for technical help, and Daniel Mrozek, Medical English Service, for editorial assistance. *Grant Support:* This work was supported in part by a grant-in-aid from the National Cancer Center Research and Development Fund (4), a grant-in-aid from the Ministry of Health, Labor, and Welfare for Third Term Comprehensive Control Research for Cancer, and a Grant-in-Aid for Scientific Research (B) (24390269).

Appendix A. Supplementary data

Supplementary data associated with this article can be found, in the online version, at http://dx.doi.org/10.1016/j.ejca.2014.01.023.

References

[1] Brodeur GM. Neuroblastoma: biological insights into a clinical enigma. Nat Rev Cancer 2003;3:203–16.

[2] Praml C, Finke LH, Herfarth C, Schlag P, Schwab M, Amler L. Deletion mapping defines different regions in 1p34.2-pter that may harbor genetic information related to human colorectal cancer. Oncogene 1995;11:1357–62.

[3] Nagai H, Negrini M, Carter SL, et al. Detection and cloning of a common region of loss of heterozygosity at chromosome 1p in breast cancer. Cancer Res 1995;55:1752–7.

[4] Smith JS, Perry A, Borell TJ, et al. Alterations of chromosome arms 1p and 19q as predictors of survival in oligodendrogliomas, astrocytomas, and mixed oligoastrocytomas. J Clin Oncol 2000;18:636–45.

[5] Yang J, Du X, Lazar AJ, et al. Genetic aberrations of gastrointestinal stromal tumors. Cancer 2008;113:1532–43.

[6] Maris JM, Weiss MJ, Guo C, et al. Loss of heterozygosity at 1p36 independently predicts for disease progression but not decreased overall survival probability in neuroblastoma patients: a Children's Cancer Group study. J Clin Oncol 2000;18:1888–99.

[7] Martinsson T, Sjöberg RM, Hedborg F, Kogner P. Deletion of chromosome 1p loci and microsatellite instability in neuroblastomas analyzed with short-tandem repeat polymorphisms. Cancer Res 1995;55:5681–6.

[8] White PS, Thompson PM, Gotoh T, et al. Definition and characterization of a region of 1p36.3 consistently deleted in neuroblastoma. Oncogene 2005;24:2684–94.

[9] Hogarty MD, Winter CL, Liu X, et al. No evidence for the presence of an imprinted neuroblastoma suppressor gene within chromosome sub-band 1p36.3. Cancer Res 2002;62:6481–4.

[10] Rountree MR, Bachman KE, Baylin SB. DNMT1 binds HDAC2 and a new co-repressor, DMAP1, to form a complex at replication foci. Nat Genet 2000;25:269–77.

[11] Negishi M, Chiba T, Saraya A, Miyagi S, Iwama A. Dmap1 plays an essential role in the maintenance of genome integrity through the DNA repair process. Genes Cells 2009;14:1347–57.

[12] Penicud K, Behrens A. DMAP1 is an essential regulator of ATM activity and function. Oncogene 2014;33:525–31.

[13] Takenobu H, Shimozato O, Nakamura T, et al. CD133 suppresses neuroblastoma cell differentiation via signal pathway modification. Oncogene 2011;30:97–105.

[14] Lavin MF. Ataxia-telangiectasia: from a rare disorder to a paradigm for cell signalling and cancer. Nat Rev Mol Cell Biol 2008;9:759–69.

[15] James HD. Topoisomerase II inhibitors: anthracyclines. In: Chabner BA, Longo DL, editors. Cancer chemotherapy and biotherapy: principles and practice. Philadelphia: Lippincott Williams & Wilkins, a Wolters Kluwer Business; 2011. p. 356–91.

[16] Shi Y, Takenobu H, Kurata K, et al. HDM2 impairs Noxa transcription and affects apoptotic cell death in a p53/p73-dependent manner in neuroblastoma. Eur J Cancer 2010;46:2324–34.

[17] Hu H, Du L, Nagabayashi G, Seeger RC, Gatti RA. ATM is down-regulated by N-Myc-regulated microRNA-421. Proc Natl Acad Sci U S A 2010;107:1506–11.

[18] Fulda S, Lutz W, Schwab M, Debatin KM. MycN sensitizes neuroblastoma cells for drug-induced apoptosis. Oncogene 1999;18:1479–86.

[19] Evan GI, Littlewood TD. The role of c-myc in cell growth. Curr Opin Genet Dev 1993;3:44–9.

[20] Schwab M, Alitalo K, Klempnauer KH, et al. Amplified DNA with limited homology to myc cellular oncogene is shared by human neuroblastoma cell lines and a neuroblastoma tumour. Nature 1983;305:245–8.

[21] Gustafson WC, Weiss WA. Myc proteins as therapeutic targets. Oncogene 2010;29:1249–59.

[22] Campaner S, Amati B. Two sides of the Myc-induced DNA damage response: from tumor suppression to tumor maintenance. Cell Div 2012;7:6.

[23] Derheimer FA, Kastan MB. Multiple roles of ATM in monitoring and maintaining DNA integrity. FEBS Lett 2010;584:3675–81.

[24] Petroni M, Veschi V, Prodosmo A, et al. MYCN sensitizes human neuroblastoma to apoptosis by HIPK2 activation through a DNA damage response. Mol Cancer Res 2011;9:67–77.

[25] Swift M, Reitnauer PJ, Morrell D, Chase CL. Breast and other cancers in families with ataxia-telangiectasia. N Engl J Med 1987;316:1289–94.

[26] Vogan K, Bernstein M, Leclerc JM, Brisson L, Brossard J, Brodeur GM, et al. Absence of p53 gene mutations in primary neuroblastomas. Cancer Res 1993;53:5269–73.

[27] Tweddle DA, Malcolm AJ, Bown N, Pearson AD, Lunec J. Evidence for the development of p53 mutations after cytotoxic therapy in a neuroblastoma cell line. Cancer Res 2001;61:8–13, http://cancerres.aacrjournals.org/content/61/1/8.long.

Published OnlineFirst May 15, 2014; DOI: 10.1158/0008-5472.CAN-14-0241

Molecular and Cellular Pathobiology

Cancer Research

Flotillin-1 Regulates Oncogenic Signaling in Neuroblastoma Cells by Regulating ALK Membrane Association

Arata Tomiyama[1,3], Takamasa Uekita[1,4], Reiko Kamata[1], Kazuki Sasaki[5], Junko Takita[2], Miki Ohira[6], Akira Nakagawara[7], Chifumi Kitanaka[8], Kentaro Mori[3], Hideki Yamaguchi[1], and Ryuichi Sakai[1]

Abstract

Neuroblastomas harbor mutations in the nonreceptor anaplastic lymphoma kinase (ALK) in 8% to 9% of cases where they serve as oncogenic drivers. Strategies to reduce ALK activity offer clinical interest based on initial findings with ALK kinase inhibitors. In this study, we characterized phosphotyrosine-containing proteins associated with ALK to gain mechanistic insights in this setting. Flotillin-1 (FLOT1), a plasma membrane protein involved in endocytosis, was identified as a binding partner of ALK. RNAi-mediated attenuation of FLOT1 expression in neuroblastoma cells caused ALK dissociation from endosomes along with membrane accumulation of ALK, thereby triggering activation of ALK and downstream effector signals. These features enhanced the malignant properties of neuroblastoma cells *in vitro* and *in vivo*. Conversely, oncogenic ALK mutants showed less binding affinity to FLOT1 than wild-type ALK. Clinically, lower expression levels of FLOT1 were documented in highly malignant subgroups of human neuroblastoma specimens. Taken together, our findings suggest that attenuation of FLOT1-ALK binding drives malignant phenotypes of neuroblastoma by activating ALK signaling. *Cancer Res; 74(14); 3790–801. ©2014 AACR.*

Introduction

Anaplastic lymphoma kinase (ALK) is a receptor tyrosine kinase (RTK) that is rather specifically expressed in the nervous system during development in mice (1). ALK was first identified in anaplastic large cell lymphoma as the fusion protein NPM-ALK caused by chromosomal translocation (2). Recently, ALK was highlighted as a therapeutic target of several cancers such as non–small cell lung cancers and colon cancers, which possess oncogenic fusion ALK proteins such as EML4-ALK (3–6). Genetic alterations of ALK have also been identified in cell lines and clinical samples of neuroblastoma, which consist of gene amplifications, activating mutations, or N-terminus truncations (7–12). Activated ALK proteins in neuroblastoma are distinct from other tumors as for the point that they retain the transmembrane domain. The survival of neuroblastoma cells with activated ALK is dependent on the ALK protein in some cases, which highlights the so called oncogene addiction to activated ALK (13).

Neuroblastoma is one of the most refractory solid tumors in children with 5-year survival rates of less than 40% following conventional treatments (14–16). To this end, clinical trials involving patients with neuroblastoma and ALK inhibitors such as crizotinib have already begun (17). However, it was reported that neuroblastoma harboring certain types of activation mutations of ALK show greater resistance to the ALK inhibitors (18) and that there are differences in the malignancy grades among neuroblastoma cases with mutant ALK depending on the type of mutations (19, 20). Therefore, further investigation is necessary to elucidate what aspects of the mutant ALK protein determine the clinicopathological features of neuroblastoma.

As ALK is a RTK, it is essential to understand the signal transduction pathways that mediate the activation of this kinase. In addition to the common downstream mediators of RTKs, such as Akt, Erk, and STAT3, we have shown the critical role of ShcC as a binding partner of ALK in neuroblastoma (21, 22). Further identification of the tyrosine-phosphorylated binding partners of ALK and analysis of their functions in neuroblastoma will aid understanding of the unique oncogenic roles of ALK signaling.

Flotillin-1 (FLOT1) is a plasma membrane lipid raft-localizing protein that is involved in internalization of membrane-localizing proteins into the cytosol by endocytosis. In addition, FLOT1 plays a role in the regulation of actin organization and neuronal regeneration (23, 24), and phosphorylation of FLOT1

Authors' Affiliations: [1]Division of Metastasis and Invasion Signaling, National Cancer Center Research Institute; [2]Department of Cell Therapy and Transplantation Medicine, Graduate School of medicine, The University of Tokyo, Tokyo; [3]Department of Neurosurgery, National Defense Medical College, Saitama; [4]Department of Applied Chemistry, National Defense Academy, Kanagawa; [5]Department of Molecular Pharmacology, National Cerebral and Cardiovascular Center Research Institute, Osaka; [6]Divisions of Cancer Genomics and [7]Biochemistry and Innovative Cancer, Chiba Cancer Center Research Institute, Chiba; and [8]Department of Molecular Cancer Science, Yamagata University School of Medicine, Yamagata, Japan

Note: Supplementary data for this article are available at Cancer Research Online (http://cancerres.aacrjournals.org/).

Corresponding Author: Ryuichi Sakai, Division of Metastasis and Invasion Signaling, National Cancer Center Research Institute, 5-1-1, Tsukiji, Chuo-ku, Tokyo 104-0045, Japan. Phone: 81-3-3542-2511; Fax: 81-3-3542-8170; E-mail: rsakai@ncc.go.jp

doi: 10.1158/0008-5472.CAN-14-0241